

# Error-related electrocorticographic activity in humans during continuous movements

Tomislav Milekovic<sup>1,2,3</sup>, Tonio Ball<sup>1,4</sup>, Andreas Schulze-Bonhage<sup>1,4</sup>,  
Ad Aertsen<sup>1,5</sup> and Carsten Mehring<sup>1,2,3</sup>

<sup>1</sup> Bernstein Center Freiburg, University of Freiburg, Hansastr. 9A, 79104 Freiburg, Germany

<sup>2</sup> Faculty of Biology, Institute of Biology I, University of Freiburg, Hauptstr. 1, 79104 Freiburg, Germany

<sup>3</sup> Department of Bioengineering and Department of Electrical and Electronic Engineering,  
South Kensington Campus, Imperial College London, SW7 2AZ London, UK

<sup>4</sup> Epilepsy Center, University Medical Center Freiburg, Breisacher Straße 64, 79106 Freiburg, Germany

<sup>5</sup> Faculty of Biology, Institute of Biology III, University of Freiburg, Schaezlestrasse 1, 79104 Freiburg, Germany

E-mail: [t.milekovic@imperial.ac.uk](mailto:t.milekovic@imperial.ac.uk)

Received 24 October 2011


Accepted for publication 12 December 2011

Published 13 February 2012

Online at [stacks.iop.org/JNE/9/026007](http://stacks.iop.org/JNE/9/026007)

## Abstract

Brain-machine interface (BMI) devices make errors in decoding. Detecting these errors online from neuronal activity can improve BMI performance by modifying the decoding algorithm and by correcting the errors made. Here, we study the neuronal correlates of two different types of errors which can both be employed in BMI: (i) the execution error, due to inaccurate decoding of the subjects' movement intention; (ii) the outcome error, due to not achieving the goal of the movement. We demonstrate that, in electrocorticographic (ECoG) recordings from the surface of the human brain, strong error-related neural responses (ERNRs) for both types of errors can be observed. ERNRs were present in the low and high frequency components of the ECoG signals, with both signal components carrying partially independent information. Moreover, the observed ERNRs can be used to discriminate between error types, with high accuracy ( $\geq 83\%$ ) obtained already from single electrode signals. We found ERNRs in multiple cortical areas, including motor and somatosensory cortex. As the motor cortex is the primary target area for recording control signals for a BMI, an adaptive motor BMI utilizing these error signals may not require additional electrode implants in other brain areas.

 Online supplementary data available from [stacks.iop.org/JNE/9/026007/mmedia](http://stacks.iop.org/JNE/9/026007/mmedia)

## 1. Introduction

Current brain-machine interface (BMI) devices make errors in decoding. Decoding errors can be recognized by the subject and can evoke an error-related neural response (ERNR). Such ERNRs could be utilized in two ways to improve the performance of a BMI: (1) to correct the error that was made and (2) to modify the decoding algorithm to decrease decoding errors in the future. The first strategy has already been applied in on-line BMI studies (Schalk *et al* 2000, Blankertz *et al* 2003, Parra *et al* 2003), but thus far only in trial-based task

designs. However, many powerful BMIs, such as the brain control of a prosthetic arm (Carmenta *et al* 2003, Hochberg *et al* 2006, Velliste *et al* 2008) and the brain control of a computer cursor (Serruya *et al* 2002, Taylor *et al* 2002, Hochberg *et al* 2006) use continuous movement control of the effector. The principal feasibility of the second strategy has, thus far, only been demonstrated in computer simulations applying decoding algorithms which adapt using error signals (Rotermund *et al* 2006, Blumberg *et al* 2007).

Both strategies for improving the performance of BMIs require appropriate ERNRs. Most previous ERNR



**Figure 1.** Application of neuronal error signals to improve the performance of a continuous BMI control. Subjects intend cursor movements in a given direction (white arrow). If the decoding is correct, the cursor performs the intended movement and no neuronal error signal is elicited in a subject. If there is a discrepancy between the intended and the decoded movement, an ERNR can be elicited. If the ERNR is detected by the BMI system, the decoding algorithm can be adapted to reduce the number of decoding errors in the future.

studies concentrated on trial-based tasks with human electroencephalogram (EEG). Several types of ERNRs were reported: response error-related negativity (rERN) (Falkenstein *et al* 1991, Gehring *et al* 1993), feedback error-related negativity (fERN) (Miltner *et al* 1997), observation error potential (oErrP) (van Schie *et al* 2004) and interaction error potential (iErrP) (Ferreze and del R Millan 2008).

By contrast, only a small number of studies investigated ERNRs in continuous movement tasks. Again, different types of errors in continuous tasks were reported: target error in functional magnetic resonance imaging (fMRI; Diedrichsen *et al* 2005), execution error in fMRI (Diedrichsen *et al* 2005) and outcome error in EEG (Krigolson *et al* 2008). Target errors occur when the movement environment goes through unexpected changes, such as a target jump. Execution errors occur when the ongoing motor commands result in an unexpected movement, due to changes in the movement dynamics or kinematics. Such error occurs in BMI when, for example, the decoding algorithm decodes incorrect movements and, hence, the prosthesis does not perform the

intended movement (figure 1). If the difference between the intended and the decoded movement is large enough, it can be recognized by the subject and evoke an execution ERNR. Finally, an outcome error appears when the desired goal of a movement is not achieved. Such error would occur in BMI when the prosthesis reaches a wrong target.

Diedrichsen *et al* (2005) found fMRI correlates of execution errors and did not investigate outcome errors. Moreover, due to the low temporal resolution, fMRI would only allow for rather slow BMI control. Krigolson *et al* (2008) observed EEG correlates of outcome errors but did not address the question of execution errors.

Here, we show that both execution and outcome ERNRs can be observed and differentiated in neuronal signals recorded directly from the surface of the human brain (electrocorticogram, ECoG; Cooper *et al* 1965, Leuthardt *et al* 2004, Schalk *et al* 2007, Pistohl *et al* 2008, Ball *et al* 2009a, 2009b, Kubanek *et al* 2009, Miller *et al* 2009, Chao *et al* 2010, Krusienski *et al* 2011) during a continuous movement task, similar to typical BMI control tasks. The semi-invasive

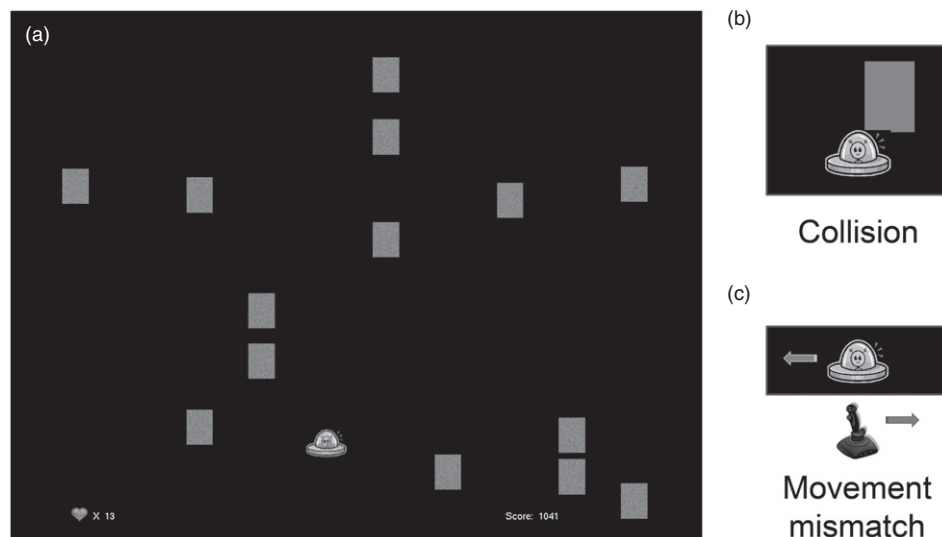


**Figure 2.** (a), A picture of the paradigm as seen by the subjects. Subjects played a video game in which they moved a spaceship in the horizontal direction (left–right) to evade the blocks dropping from above. Every time the spaceship collided with a block (collision event; (b)), one life was lost. From time to time, the spaceship moved in the opposite direction to the joystick movement for 500 ms (movement mismatch event; (c)). Performance of the subject was measured by a score is shown in the bottom-right of the screen. The number of remaining lives is shown in the bottom-left corner. The game (and the experimental session) ended when all lives were lost.

ECoG is an attractive recording technique for BMIs as it does not require the implantation of electrodes into the cortex and offers a higher spatial and spectral resolution than the non-invasive EEG and MEG.

We found ERNRs above different cortical areas, including motor cortex. Both low pass filtered ECoG signals and high gamma ECoG signals yielded execution and outcome ERNRs, with both signal components carrying partially independent information. In addition, execution and outcome ERNRs can be differentiated with high decoding accuracy, even based on the responses from only one electrode.

## 2. Methods

### 2.1. Task

Subjects (S) played a simple video game in which they controlled a spaceship with a small analogue joystick on a gamepad (Logitech® Rumblepad™ 2, Logitech Europe S.A., Morges, Switzerland) in the horizontal dimension (left to right; figure 2(a); supplementary movie 1 available from [stacks.iop.org/JNE/9/026007/mmedia](http://stacks.iop.org/JNE/9/026007/mmedia)). The task was to evade blocks dropping from the top of the screen at a constant speed. The game was challenging enough so that the spaceship collided with a block from time to time (collision event, figure 2(b), mean and standard error of the mean, sem, of time between events: S1:  $26.25 \pm 1.80$  s, S2:  $38.57 \pm 3.11$  s, S3:  $47.62 \pm 4.80$  s, S4:  $15.83 \pm 0.96$  s). After the collision event, the spaceship and all blocks stopped moving for 2 s, to allow subjects to recognize the collision. Afterwards all blocks disappeared and the spaceship started to move again.

Occasionally, the spaceship moved in the opposite direction to the joystick movement for the duration of 500 ms (movement mismatch event, figure 2(c), mean and sem of time between events: S1:  $18.46 \pm 1.08$  s, S2:  $13.17 \pm 0.49$  s, S3:  $30.36 \pm 2.52$  s, S4:  $24.79 \pm 2.33$  s). Movement

mismatch event was introduced to study neuronal responses to execution errors. To make these events noticeable and to also make them look as part of the natural movement, they were triggered only when the following conditions were fulfilled: (i) the spaceship was not close to the paradigm borders, (ii) the joystick position was between 60% and 70% of the maximum deflection, (iii) the joystick velocity (first derivative of joystick deflection) was in the direction of the joystick deflection, and (iv) the blocks were not too close to the spaceship. Condition (iv) was introduced to minimize the chance of a block collision following an unexpected change in the spaceship movement direction due to the movement mismatch event. For the first two subjects, condition (iii) was not imposed and a movement mismatch event was triggered only during joystick movements to the right.

Points were awarded for moving the spaceship, and subjects were instructed to gather as many points as possible. The number of points increased linearly with the distance the spaceship travelled. To control the attention of the subjects the colour of the spaceship changed between red and blue at random instants, events which subjects were asked to orally report. Subjects correctly reported colour changes except on a very few occasions. For the last two subjects, screen freeze events were added where, at a random instant (mean time between events: S3:  $36.67 \pm 0.89$  s, S4:  $36.15 \pm 1.09$  s), the spaceship and all blocks stopped moving for 2 s in the same manner as after a collision event. We added screen freeze events to serve as a visual and surprise control (see section 2.2).

To avoid mixing between neuronal responses to different events, all triggered events (movement mismatch, screen freeze and colour change) were triggered at least 2 s away from the last preceding event of any kind (movement mismatch, screen freeze, colour change, collision, paradigm restart after collision and end of screen freeze event). This procedure was not enough to remove the mixing completely, since the timing

**Table 1.** Number of recorded sessions and events for each of the subjects. For subjects S1 and S2 freeze event was not implemented in the experiment.

| Sessions |   | Collision events |       | Mismatch events |       | Colour ch. events |       | Freeze events |       |
|----------|---|------------------|-------|-----------------|-------|-------------------|-------|---------------|-------|
|          |   | All              | Clean | All             | Clean | All               | Clean | All           | Clean |
| S1       | 8 | 160              | 120   | 195             | 155   | 101               | 63    | 0             | 0     |
| S2       | 4 | 80               | 38    | 227             | 185   | 125               | 85    | 0             | 0     |
| S3       | 4 | 80               | 51    | 121             | 92    | 139               | 134   | 109           | 109   |
| S4       | 6 | 120              | 87    | 71              | 38    | 71                | 62    | 62            | 62    |

of the collision events could not be controlled. Therefore, events were classified after the experiment as ‘clean’ if no other event was closer than 2 s.

Subjects started the game with 20 ‘lives’. Each time the spaceship collided with a block, the number of ‘lives’ was reduced by one. When the number of ‘lives’ reached zero, the game, together with the recording session, ended. Recording sessions of all subjects lasted between 5 and 24 min. There were no auditory stimuli presented during the experiment. A summary of the number of recorded sessions and the number of recorded events is given in table 1.

## 2.2. Error and control events

To play the game as long as possible and, thereby, earn more points, subjects needed to evade hitting the blocks falling down from the top. Therefore, every collision event that occurred presented a clear disadvantage in reaching the goal of the game. Thus, collision events reflect outcome errors. During the movement mismatch event, the ongoing motor command resulted in an unexpected movement due to the change in movement kinematics. Thus, movement mismatch events reflect execution errors.

Neuronal responses triggered on collision or movement mismatch events might also, partly or entirely, be the result of specific behaviour and/or visual inputs related to the error event, rather than only the neuronal response to the errors themselves. Hence, to identify ERNRs, the responses to collision or movement mismatch events need to be compared to the neuronal responses during behaviour and visual stimuli specific to the collision or movement mismatch events, but without the error context. Any significant deviation between the two responses may then be assumed to present an ERNR. We considered the following controls:

- (1) Movement control: All subjects in this study had implants over the motor and the somatosensory-related areas. Therefore, neuronal responses to collision or movement mismatch events can be movement related. To minimize the influence of movement-related neuronal responses (MRNR), subjects were asked to relax and perform a minimum amount of movement. The only movements they had to perform were thumb movements to move the joystick. Thumb movements were always carried out with the thumb contra-lateral to the brain hemisphere where the electrode grid was located. Subjects occasionally made eye movements to observe what was happening on the screen. To remove the influence of the eye and thumb movements from the recorded neuronal signals, MRNR

were removed using the subtraction method described in section 2.4.3.

- (2) Visual control: Specific visual feedback provided by the paradigm can generate part of the neuronal response triggered by collision or movement mismatch events. Screen freeze events presented identical visual stimuli as collision events, the only difference being that, in the screen freeze event, the spaceship did not touch one of the blue blocks on the screen. Therefore, screen freeze events were used as a visual control for the collision events. This visual control was implemented for S3 and S4 only.
- (3) Surprise control: Great care was taken to make movement mismatch events look like part of the undisturbed spaceship movement, unrecognizable from watching the paradigm only. Therefore, no visual stimulus was specific to the movement mismatch events. On the other hand, movement mismatch events could not be predicted by the subject and, hence, could trigger a surprise-related neuronal response. Therefore, we used the freeze events, which could also not be predicted by the subject, as a control event for the movement mismatch events. This surprise control was implemented for S3 and S4 only.

## 2.3. Subjects and recordings

Four subjects (three male, one female) suffering from intractable pharmaco-resistant epilepsy voluntarily participated in the study after having given their informed consent. The study was approved by the University Hospital’s Ethics Committee.

For pre-neurosurgical epilepsy diagnosis, the subjects were implanted with an  $8 \times 8$  grid of subdural surface electrodes covering parts of the primary and pre-motor cortex (figure 3). In addition, S1, S2 and S3 had the following implanted electrodes: S1 had two strips, with six electrodes each, implanted subdurally over the prefrontal cortex and four strips, with four electrodes each, implanted subdurally in the interhemisphere region touching the left hemisphere. S2 had two strips, with six electrodes each, implanted subdurally over the bottom of the cerebellum and four strips, with four electrodes each, implanted subdurally over the temporal and prefrontal cortices. S3 had two strips, with four electrodes each, implanted subdurally over the prefrontal cortex. The sites of all electrode implantations were exclusively based on the requirements of the clinical evaluation. In S2, the signals from the top row of electrodes in the grid implant and from one of the strips over the bottom of the cerebellum (TbD) were not recorded due to the limited number (128) of



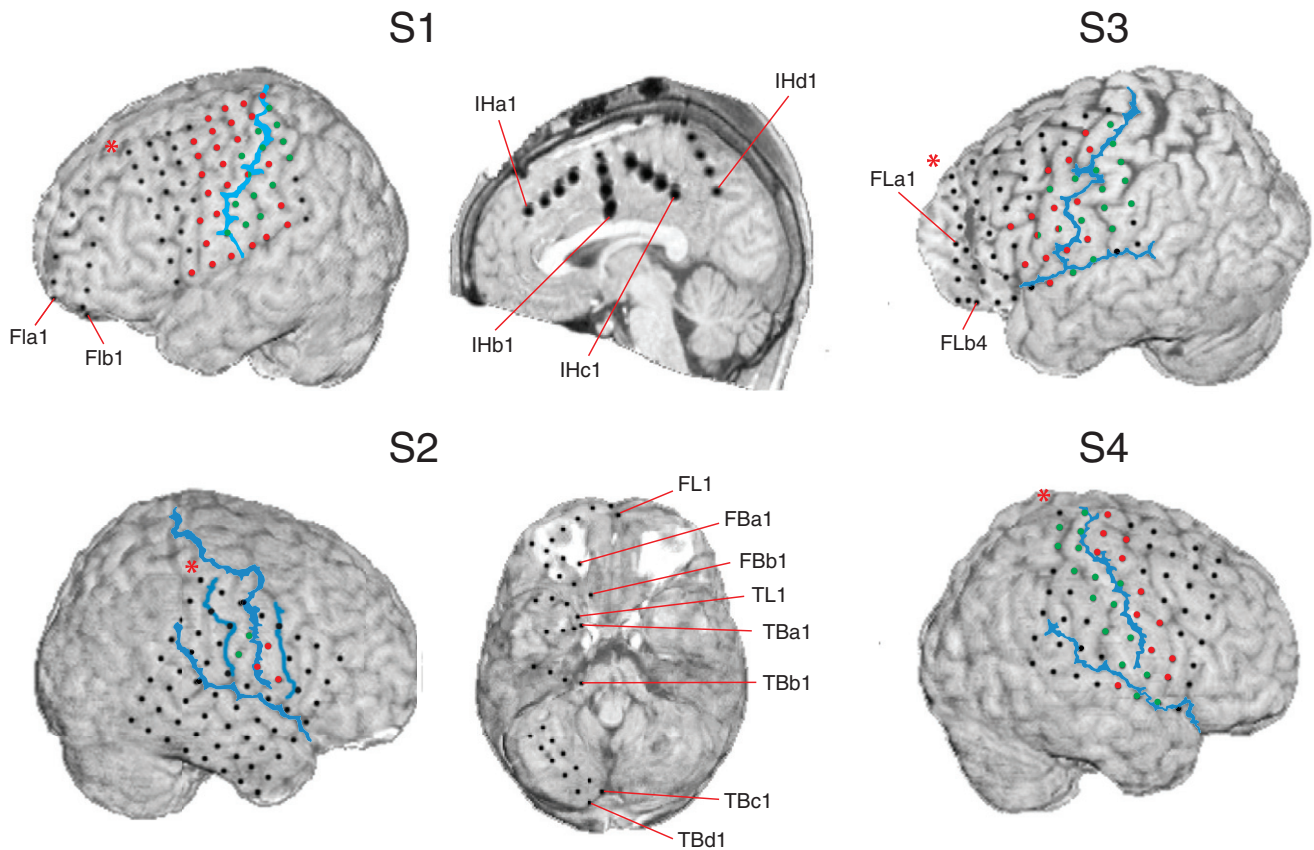


**Figure 3.** Locations of implanted electrodes (red, green and black circles). Electrode positions are reconstructed from the post-implantation MRI scan and positioned over the pre-implantation MRI scan (Kovalev *et al* 2005). For S1, S3 and S4 red (green) circles represent electrodes that showed motor (somatosensory) response from electrical stimulation mapping (ESM). For S2 motor and somatosensory electrodes were determined from sulci reconstruction. Central sulci, Sylvian fissures and, for S2 only, pre- and post-central sulcus are shown as blue lines. These have been drawn by hand to resemble sulci reconstruction from the post-implantation MRI scan. S1 was implanted with an  $8 \times 8$  ECoG grid over the parts of frontal and parietal lobe, two 6 electrode ECoG strips over the frontal lobe (FLa and FLb) and four 4 electrode ECoG strips inter-hemispherically (IHa, IHb, IHc and IHd). S2 was implanted with an  $8 \times 8$  ECoG grid over parts of temporal, parietal and frontal lobe, two 6 and three 4 electrode ECoG strips on the basal temporal cortex (TL, TBa, TBb, TBc and TBd) and two 4 electrode and one 6 electrode ECoG strips on the basal frontal lobe (FL, FBa and FBb). In S2 no recordings were made from the top row of the  $8 \times 8$  electrode grid and from the TBd ECoG strip. S3 was implanted with an  $8 \times 8$  ECoG grid over the parts of frontal and parietal lobe and two 4 electrode ECoG strips (FBa and FBb) over the frontal lobe. S4 was implanted with an  $8 \times 8$  ECoG grid over parts of parietal and frontal lobe. In all pictures the red star marks the edge of the electrode grid corresponding to the top-left corner in the SNR distribution pictures shown in figure 9.

available channels in the recording system. In addition to the subdural surface electrodes, additional intracortical electrodes were implanted and 22 channels of EEG, two to four channels of electrooculogram (EOG), and single electrocardiogram (ECG) and electromyogram (EMG) channels were recorded simultaneously. Signals from the intracortical, EEG, ECG and EMG electrodes were not analysed in this study.

Recordings from all electrodes were digitized at 256 Hz sampling rate for S1 and S2 and at 1024 Hz sampling rate for S3 and S4, in all cases using a clinical ac amplifier (Brainbox EEG-1164 amplifier, Braintronics BV, Almere, Netherlands). No analogue filters were used during the data acquisition. Power line frequency was 50 Hz. Experiment control and paradigm presentation was performed using our own laboratory software. Subsequent data analysis was performed using MATLAB (MATLAB version 7.4-7.11, Natick, MA: The MathWorks Inc., 2007–2011).

## 2.4. Data analysis

**2.4.1. Preprocessing.** Common-average referencing for grid electrodes was made using all grid electrodes that showed no artefacts (one electrode for both S3 and S4 had to be excluded). Electrode strips above frontal cortex of S1 were re-referenced using all electrodes on those two strips. Inter-hemisphere electrodes for S1 were re-referenced using all electrodes on those four strips. For S2, electrode strips above the bottom of the cerebellum, temporal and frontal areas were re-referenced together. For S3, electrode recordings from two strips above frontal areas were re-referenced together. To correct for changes in channel offsets between sessions, the mean voltage over the entire session was subtracted for every session and for every channel after re-referencing.

**2.4.2. Signal components.** We extracted low and high frequency components of the recorded ECoG signals. To analyse the low frequency component of the signal, the

preprocessed ECoG signals were smoothed using a symmetric Savitzky–Golay filter (Savitzky and Golay 1964, Steinier *et al* 1972). The Savitzky–Golay filter is not a filter designed with a specific cut-off frequency. It is a smoothing filter that performs least-squares fitting of a polynomial of a certain order (second order in the case of our study) to the signal in a certain time window (250 ms of recorded data points in the case of our study). Even though the frequency domain properties of a Savitzky–Golay filter do not resemble that of a typical low-pass filter (Schafer 2011) a nominal 3 dB cut-off frequency can be determined and was, in our case, 7.85 Hz for S1 and S2 and 7.59 Hz for S3 and S4.

We defined a window around each event (movement mismatch, screen freeze, colour change, collision), starting 3 s before each event and lasting until 3 s after each event. The signals outside all of these windows were used as baseline activity. To enable a clear comparison to baseline, the average baseline activity was subtracted from the filtered recordings in each session for each channel. The resulting signal was defined as the low frequency component of the signal.

To analyse the high frequency component of the signal, time-resolved Fourier transformation (TRFT) using a Hamming window (333 ms window width, shifted in steps of 31 ms) was applied to the preprocessed signals, and the amplitudes were used for further analysis. To investigate event-induced changes in amplitudes and to account for the general decrease in amplitude with increasing frequency, the amplitudes of every frequency bin were normalized by dividing them by the average baseline amplitude of the same frequency bin in the respective session. Afterwards, the average amplitude across a frequency range was computed for further analysis: for S1 and S2 over the frequency band from 60 to 128 Hz (Nyquist frequency), for S3 and S4 over the frequency band from 60 to 200 Hz (figure 4).

MRNR were then subtracted from both signal components as described in the following.

**2.4.3. MRNR subtraction.** As described above, we considered that thumb and eye movements might be correlated with error events. If so, parts of the neuronal responses, correlated with error events, might not be evoked by error events but by accompanying eye and thumb movements.

To remove the movement-related component of the neuronal response following a mismatch or a collision event, we derived a model relating the signals to the movements using only non-event data (i.e. all data that were at least 1 s before and 3 s after any event) and then subtracted the signals predicted by this model for the movements during the events from the recorded event-related signals. The required thumb movements were tracked indirectly through the joystick movements, while the required eye movements were tracked through the horizontal and vertical EOG.

Two types of models were considered, linear and nonlinear models. Linear models assumed a linear relationship between the neuronal response at time  $t$ ,  $Y_{CH}(t)$ , and the joystick position  $X$ , the absolute joystick position  $|X|$ , the joystick velocity  $V$ , the absolute joystick velocity  $|V|$ , the horizontal EOG *heog* and the vertical EOG *veog* at different time points around  $t$ :

$$\Delta t_i = \begin{cases} 0 & \text{for } N = 1 \\ \left( \frac{i-1}{N-1} - \frac{1}{2} \right) \cdot L & \text{for } N > 1 \end{cases}$$

$$Y_{CH}(t) = a_0^{CH} + \sum_{i=1}^N b_i^{CH} X(t + \Delta t_i) + \sum_{i=1}^N c_i^{CH} |X(t + \Delta t_i)| \\ + \sum_{i=1}^N d_i^{CH} V(t + \Delta t_i) + \sum_{i=1}^N e_i^{CH} |V(t + \Delta t_i)| \\ + \sum_{i=1}^N f_i^{CH} heog(t + \Delta t_i) + \sum_{i=1}^N g_i^{CH} veog(t + \Delta t_i),$$

where  $N$  is the number of used data points for each movement parameter,  $L$  is the length of the movement information provided to the decoder,  $a_0^{CH}, b_1^{CH}, \dots, b_N^{CH}, c_1^{CH}, \dots, c_N^{CH}, e_1^{CH}, \dots, e_N^{CH}, f_1^{CH}, \dots, f_N^{CH}, g_1^{CH}, \dots, g_N^{CH}$  are the model coefficients and  $\Delta t_i$  are the time lags relative to the neuronal response. Time lags  $\Delta t_i$  were such that the times of the  $N$  movement data points entering the model were spread equidistantly on a time stretch of length  $L$  centred on the time  $t$ .

Nonlinear models try to address a possibly nonlinear relationship between the neuronal response at time  $t$ ,  $Y_{CH}(t)$ , and the joystick position  $X$ , the joystick velocity  $V$ , the horizontal EOG *heog* and the vertical EOG *veog* at different time points around  $t$ :

$$Y_{CH}(t) = F(X(t + \Delta t_i), \dots, V(t + \Delta t_i), \dots, heog \\ \times (t + \Delta t_i), \dots, veog(t + \Delta t_i), \dots).$$

Time lags  $\Delta t_i$  were the same as used in the linear model. Absolute position and absolute velocity were not used since nonlinear modelling is able to account for the nonlinear absolute value transformation. In the case of the linear models, for a certain value of  $L$  and  $N$ , the model coefficients can be fitted by linear least-squares regression. For nonlinear models more complex algorithms have to be used. Here we used the epsilon-SVR algorithm, part of the LIBSVM library (Fan *et al* 2005).

Optimal values of  $L$  and  $N$  are not known *a priori*: if many time lags are used (high value of  $N$ ), the model might overfit the data and, therefore, the model predictions might poorly generalize due to inaccurate model coefficients. If only a few time lags are used (low value of  $N$ ), the model predictions might also generalize poorly as not all available information for predicting the movement-related neuronal responses is incorporated into the model. Similarly, if the time stretch ( $L$ ) is too small, the information contained in points further away in time would not be used, whereas nearby points might contain redundant information. Using large time stretches, on the other hand, might result in missing information contained between two time lags. Therefore, we needed to determine the values of  $L$  and  $N$  which yield optimal model prediction. To this end, we split the non-event data into two halves: the first half was used to estimate the model coefficients for certain values of  $L$  and  $N$ . These model coefficients were then used to predict the signals of the second half of the data. To determine the performance of the model, we computed  $r^2$  values between

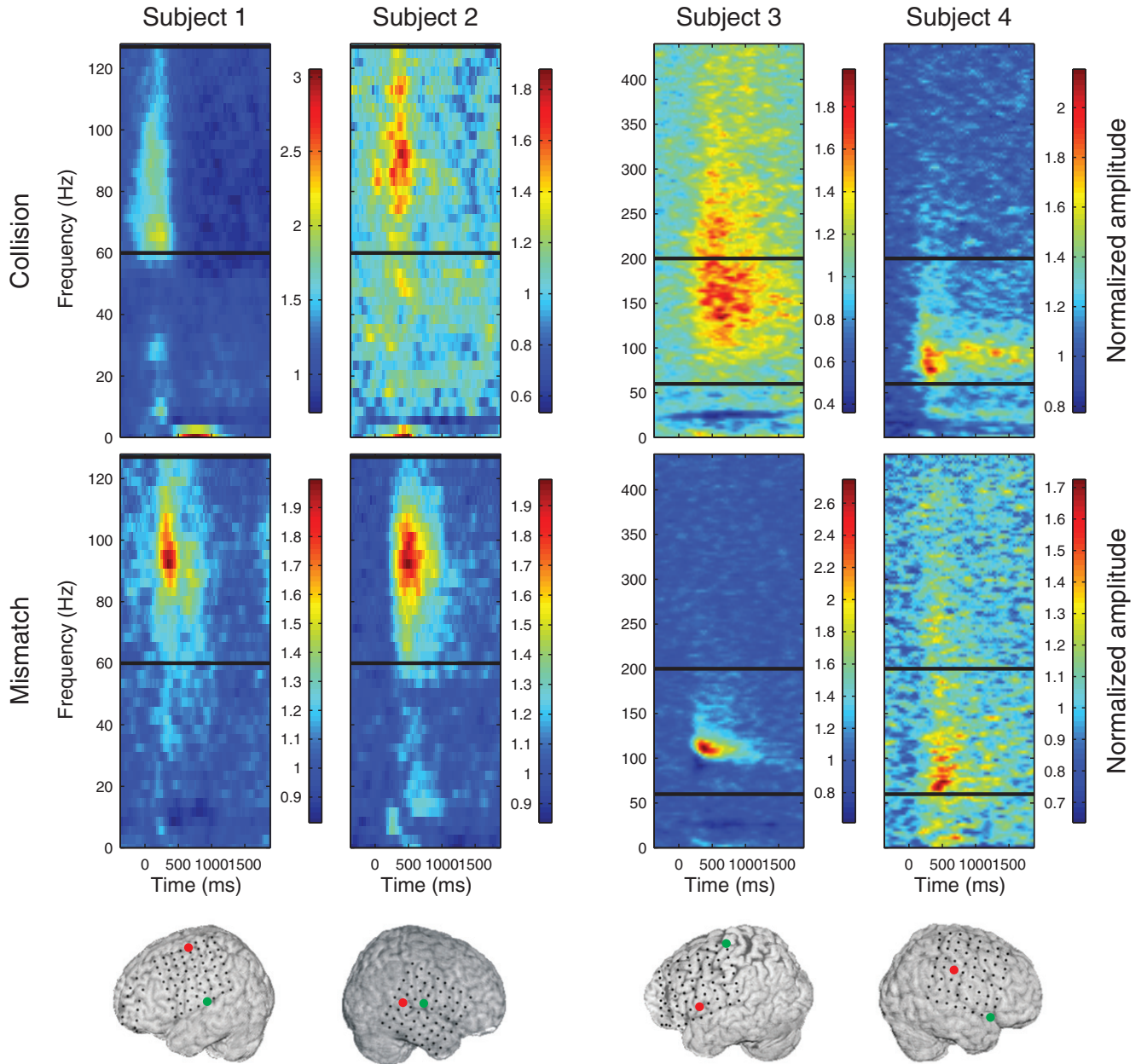


**Figure 4.** Examples of the averaged normalized spectrograms to collision and to mismatch events for one electrode for each of the subjects. Channels used as examples are marked in red for collision and green for mismatch events on the small depictions of the subjects' brains below the spectrograms. Black horizontal lines indicate the bottom and top frequencies of the band used for the high-frequency component of the signal. In S1 and S2, the upper boundary of this band was at the Nyquist frequency.

the model predictions and the real neuronal responses in the second half of the data:

$$r^2 = 1 - \frac{V(Y(t) - Y_{\text{MODEL}}(t))}{V(Y(t))}.$$

This measure was computed for different values of  $L$  (62.5, 109.4, 156.2, 203.1, 250, 375, 500, 750, 1000, 1250, 1500, 1750 and 2000 ms) and  $N$  (1, 2, 3, 4, 6, 10, 14, 18 and 22) for both linear and nonlinear models and the one yielding the highest  $r^2$  values was then used for the MRNR subtraction. These optimal values were determined for each channel individually. Channels yielding an  $r^2$  below 0.01 were considered as being not movement related; for these channels nothing was subtracted from the event-related signals.

**2.4.4. Error-related neuronal responses.** To avoid mixing of neuronal responses to different events only epochs from clean events (see section 2.1) were used for subsequent analysis. After the MRNR subtraction, the remaining signal should predominantly contain the neuronal responses to errors. Therefore, the neuronal responses to collision and mismatch events are called outcome and execution ERNRs after MRNR subtraction.

**2.4.5. Signal to noise ratio analysis.** To compare the event triggered neuronal response  $\Phi_{\text{EVENT}}$  to the baseline activity  $\Phi_{\text{BASELINE}}$  (as defined in section 2.4.2) or to the event triggered neuronal response of another event  $\Phi_{\text{EVENT2}}$ , the signal to noise



ratio (SNR) was used. Let  $n$  be the event index,  $t$  the time within the event epoch,  $m$  the index of the baseline measurement,  $E$  the expectation operator, and  $\text{std}$  the standard deviation operator. We defined the SNR as follows:

$$\begin{aligned}\mu_{\text{EVENT}}(t) &= E(\Phi_{\text{EVENT}}(n, t), n) \\ \sigma_{\text{EVENT}}(t) &= \text{std}(\Phi_{\text{EVENT}}(n, t), n) \\ \mu_{\text{BASELINE}} &= E(\Phi_{\text{BASELINE}}(m), m) \\ \sigma_{\text{BASELINE}} &= \text{std}(\Phi_{\text{BASELINE}}(m), m) \\ \text{SNR}(t)_{\text{EVENT vs BASELINE}} &= \frac{|\mu_{\text{EVENT}}(t) - \mu_{\text{BASELINE}}|}{\sigma_{\text{EVENT}}(t) + \sigma_{\text{BASELINE}}} \\ \text{SNR}(t)_{\text{EVENT1 vs EVENT2}} &= \frac{|\mu_{\text{EVENT1}}(t) - \mu_{\text{EVENT2}}(t)|}{\sigma_{\text{EVENT1}}(t) + \sigma_{\text{EVENT2}}(t)}.\end{aligned}$$

For limited numbers of trials, the SNR is positively biased (Mehring et al 2003). To correct for this, we used a bootstrap bias correction (Efron and Tibshirani 1993), with 1000 times resampling of the event data to remove this bias.

The above computations yielded, for each type of ERNR, an SNR against baseline and an SNR against the control event. Since, to detect ERNRs, we needed to differentiate them from baseline and control events, we quantified the SNR of an ERNR by the minimum among these two SNR values. This yielded one SNR value for each point in time. To describe the strength of the ERNR by a single number, we introduced the outcome SNR and the execution SNR as the maximum of these SNR values between 100 and 800 ms after the trigger.

To be able to differentiate between outcome and execution error events, outcome ERNRs have to be different from the execution ERNRs. Since outcome and execution ERNR may have different delays with respect to the trigger, we cannot directly compare these two signals. Therefore, we computed the outcome versus execution SNR as follows:

$$\begin{aligned}\text{SNR}_{\text{MAX}} &= \frac{|\mu_O(t_{O\text{max}}) - \mu_E(t_{E\text{max}})|}{\sigma_O(t_{O\text{max}}) + \sigma_E(t_{E\text{max}})}, \\ \begin{cases} t_{O\text{max}} = \max_t \arg(\mu_O(t)) \\ t_{E\text{max}} = \max_t \arg(\mu_E(t)) \end{cases} \\ \text{SNR}_{\text{MIN}} &= \frac{|\mu_O(t_{O\text{min}}) - \mu_E(t_{E\text{min}})|}{\sigma_O(t_{O\text{min}}) + \sigma_E(t_{E\text{min}})}, \\ \begin{cases} t_{O\text{min}} = \min_t \arg(\mu_O(t)) \\ t_{E\text{min}} = \min_t \arg(\mu_E(t)) \end{cases} \\ \text{SNR}_{\text{OUTCOME vs EXECUTION}} &= \max(\text{SNR}_{\text{MAX}}, \text{SNR}_{\text{MIN}})\end{aligned}$$

where  $t$  runs from 100 to 800 ms after the trigger,  $\mu_O$  is the average outcome ERNR,  $\mu_E$  is the average execution ERNR,  $\sigma_O$  is the standard deviation of the outcome ERNR across trials and  $\sigma_E$  is the standard deviation of the execution ERNR across trials.

**2.4.6. Classification analysis.** To see how well ERNRs can be differentiated from baseline activity on a single-trial basis, we performed a binary classification analysis of outcome or execution ERNRs versus baseline activity using regularized linear discriminant analysis (RLDA) (Friedman 1989). The class representing baseline activity contained all baseline

activity recordings as defined in section 2.4.2. The other class representing either outcome or execution ERNR was composed of outcome (execution) ERNRs at the time of the average outcome (execution) ERNR peak (see section 2.4.5). Only single signal components from single channels were used as inputs to the RLDA. Trials were shuffled and divided into a training set, which contained two-thirds of the data, and a test set, which contained the remaining one-third of the data. The training set was used to train the RLDA model, which was then used to classify the test set. The decoding accuracy (DA) was computed as follows:

$$\text{DA} = \frac{1}{N_{\text{class}}} \sum_{i=1}^{N_{\text{class}}} \frac{c_i}{n_i},$$

where  $N_{\text{class}}$  is the number of classes (in our case—two; outcome or execution versus baseline),  $c_i$  is the number of correctly decoded trials for a given class and  $n_i$  is the total number of trials for a given class within the test set. The regularization parameter of the RLDA was optimized on the training data by five times five-fold cross validation.

Additionally, we classified outcome versus execution ERNR using the same classification procedure as above. Instead of using only one time point to differentiate between two signals, we allowed for 1–4 points centered around the time of the ERNR peak. The number of time points and the temporal distance between the first and the last time point (between 31 and 281 ms) together with the regularization parameter of the RLDA were optimized on the training set using five times five-fold cross validation.

**2.4.7. Significance testing of neural responses.** To confirm that ERNRs were significantly different from neural responses during baseline and to freeze events the Mann–Whitney–Wilcoxon test was applied between an ERNR at every time point and the baseline activity. To avoid the autocorrelation of the low frequency component arising from the filtering procedure, we sampled low frequency component baseline activity every 250 ms and high frequency component baseline activity every 333 ms. To confirm that ERNRs were significantly different from freeze events the Mann–Whitney–Wilcoxon test was applied between an ERNR and the neuronal response to freeze events at every time point after the event trigger. Since ERNR had to be present within a limited time after the trigger, we tested the epoch of the neural response from 100 till 800 ms after the event trigger. To reduce the calculation time of the significance testing, we tested significance of the neural responses every 31 ms (roughly 32 Hz) instead of testing for every recorded time point.

Due to the large number of statistical tests, correction for multiple testing was necessary to control the number of falsely rejected null hypotheses. We used the Benjamini–Hochberg procedure (Benjamini and Hochberg 1995) with a correction for dependent statistics (Benjamini and Yekutieli 2001) to set the false discovery rate for one subject at the level of 5% for all tests. A neuronal response from a single channel/frequency component was declared significant if there was at least one time point for which the ERNR was significantly different



from the baseline and significantly different from the freeze neuronal response after the correction for multiple testing was made.

To test whether the used statistical test for the significant event responses was not detecting large number of false positives, we made 100 repetitions of the procedure for significance testing. In each repetition, we assigned random time to every event (collision, movement mismatch, freeze and colour change), respecting the rule that all paradigm triggered events (movement mismatch, freeze and colour change) have to come at least 20 s after any event (movement mismatch, screen freeze, colour change, collision, paradigm restart after collision and end of screen freeze event). To remove the MRNR, we used the same models that were used in the analysis of data using non-shuffled trigrams.

### 2.5. Neuroanatomical analysis

To determine whether the motor or the somatosensory cortex played a more distinctive role in generating ERNR, we classified electrodes into motor cortex electrodes, somatosensory cortex electrodes and other electrodes. Classification was performed combining the results of sulci identification on the post-implantation MRI scans with the results of direct cortical electrical stimulation mapping (ESM; Foerster 1931, Uematsu *et al* 1992).

Electrical cortical stimulation through the electrode grid was performed using an INOMED NS 60 stimulator (INOMED, Germany). Trains of 7 s duration consisted of 50 Hz pulses of alternating polarity square waves of 200  $\mu$ s each. The intensity of stimulation was gradually increased up to 15 mA or to the induction of sensory and/or motor phenomena. The patients were unaware of the timing of stimulation unless motor symptoms or somatosensory sensations occurred.

Electrical stimulation of by-passing paths may indeed lead to functional responses that are not directly related to the cortex under a given electrode contact. To reduce such effects, we have carried out electrical stimulation against different reference electrodes, such as directly neighbouring ones or electrodes with a large distance from the stimulated ones. As stimulation against different reference electrodes will cause different current distributions, such effects may be reduced, albeit not completely excluded, in this manner. Only effects that were consistently observed, independently of the choice of the reference electrode, were used to generate the maps shown in the paper.

Data from post-implantation MRIs provided us with the positions of central sulcus and Sylvian fissure with respect to the electrodes. The central sulcus was used to generate a border between motor and somatosensory cortex, while the Sylvian fissure was used to generate a border between the temporal lobe and the frontal and parietal lobe, containing motor and somatosensory cortex, respectively. Results of ESM were used to define a border between motor cortex and the remainder of the frontal lobe on the one hand, and somatosensory cortex and the rest of the parietal lobe on the other. S2 did not go through the ESM. Therefore, in that case, we used the pre- and

postcentral sulci, as derived from post-implantation MRI, to define the borders of the motor and the somatosensory cortex.

In addition, we used the ESM results to further classify motor and somatosensory electrodes into hand, arm, leg, ocular and oro-facial subgroups. This classification was performed solely on the basis of ESM results. S2 was excluded from this analysis since ESM was not carried out for this subject. Leg motor electrodes only existed in S1 and, for the other three subjects where ESM was performed, ocular and leg somatosensory electrodes were not found.

## 3. Results

We present our results in the following order. First we show that significant outcome and execution ERNR can be found in all subjects and that these ERNRs are widespread over the part of the cortex that we recorded from. Second, temporal distribution of ERNR peaks is presented and the reason for our choice of the time analysis window, from 100 ms after the event until 800 ms after the event, is shown to be plausible. Third, we provide the evidence that, for every subject, ERNRs can be differentiated from baseline and between each other. Next, we show the spatial distribution of the ERNRs and look whether there is a clear focus of outcome or execution ERNRs over motor or somatosensory cortex. Finally, we present the results of the classification analysis, showing that both outcome and execution ERNRs can be classified from baseline and between each other with high DA.

### 3.1. Widespread ERNRs

For the outcome error, 63% (397 out of 632; S1: 161 out of 184, S2: 92 out of 176, S3: 72 out of 144, S4: 72 out of 128) and for the execution error, 41% (259 out of 632; S1: 117 out of 184, S2: 73 out of 176, S3: 53 out of 144, S4: 16 out of 128) of channels/signal components had significant ERNR. When using shuffled times of the events, none of the channels were found significant for any of the errors and any of the signal components in all shuffles for S1 and S2. For S3 and S4, 0.03 and 0.0025 channels were found significant for any error/signal component on average. This shows that our statistical test is highly conservative and that the expected number of falsely detected ERNRs is very low.

### 3.2. ERNR latencies

To quantify the response strength we computed the SNR at the peak of the outcome or execution ERNRs within the time window from 100 to 800 ms after the error event. To verify that this window captured the majority of the responses we calculated the temporal distribution of the peaks of the ERNRs (figure 5). This distribution clearly peaks within our time window (100–800 ms). Furthermore, 90% of all ERNRs significant between 500 ms before and 1500 ms after the event were also significant within our time window. Thus, our time window captured essentially all ERNRs.

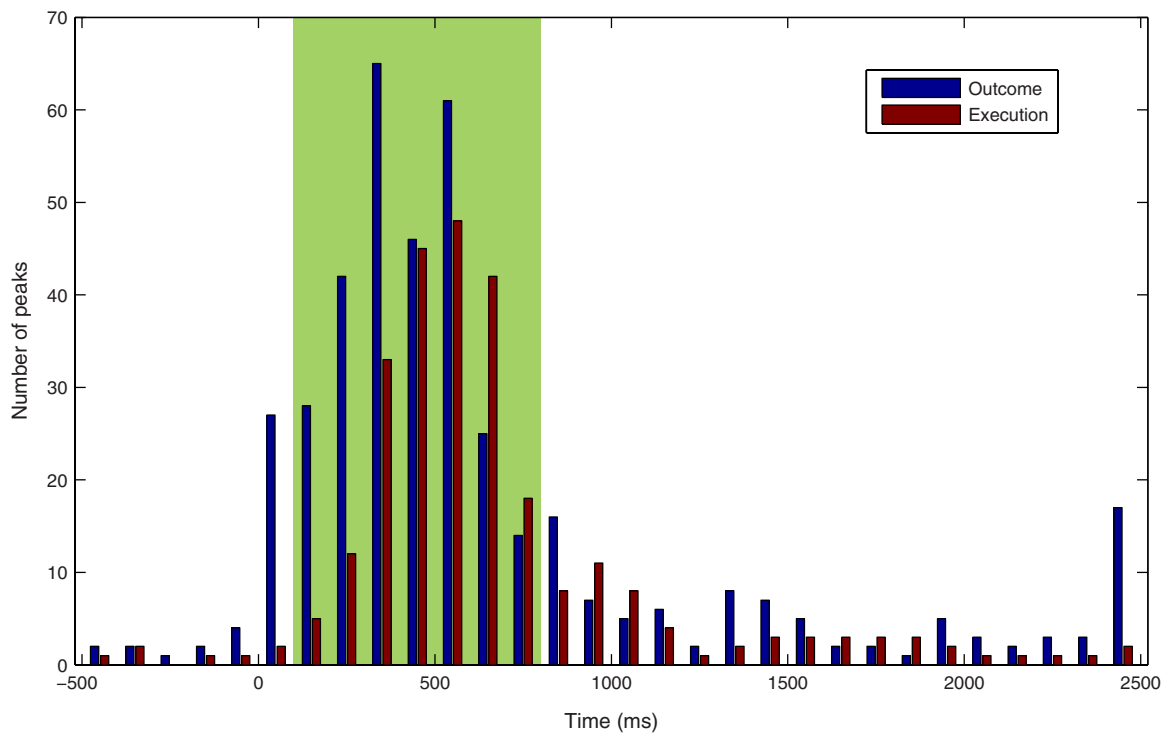


**Figure 5.** Temporal distribution of the ERNR peaks of channels/signal components with significant response when significance was checked on a window between 500 ms before till 1500 ms after the error event. Number of the outcome ERNR peaks is shown in blue, while the number of the execution ERNR peaks is shown in red. Green background depicts the time interval (100 ms after the error event until 800 ms after the error event) used to calculate the outcome and execution SNR.

### 3.3. Differentiating ERNRs from baseline and between each other

Every channel and signal component can either have a strong response to both error types (outcome and execution), a strong response to either one of the errors and a weak or no response to the other one, or a weak or no response to both errors. If a signal is strongly responsive to both errors, the outcome versus execution SNR shows whether the response to both errors is similar or dissimilar. To fully utilize all information from the ERNR, one needs to find a combination of channels/signal components for every subject that can be used to detect execution and outcome ERNRs and to differentiate between the two. This would be possible if one of the following three conditions is met: (1) separate signals with strong outcome ERNR and weak execution ERNR and with strong execution ERNR and weak outcome ERNR co-exist in the same subject, (2) one or more signals with strong but dissimilar ERNRs to execution and outcome errors co-exist in the same subject, (3) one or more signals with strong and similar ERNRs for both error events co-exist in the same subject with at least one other signal with a strong ERNR for only one of the error events.

For all subjects at least one of the required conditions was met, even when a very high threshold of  $\text{SNR} \geq 0.5$  was applied. Condition 1 was met for S3 only, condition 2 was met for all of the subjects and condition 3 was met for all subjects except S1 (see figures 6 and 7 for examples).

To be able to detect and differentiate outcome and execution errors from only one channel/signal component, high outcome SNR and high execution SNR are required simultaneously with highly different responses to both errors.

Figure 8(a) shows the outcome versus execution SNR against the minimum between outcome SNR and execution SNR for all channels and signal components for each of the subjects. Points far from the origin with regard to both axes indicate channels that can be used to detect and differentiate ERNRs. For each subject such channels/signal components were found.

In addition, information from multiple channels and signal components can be used to improve the detection of outcome and execution errors and the discrimination between the two. Figure 8(b) shows the distribution of the execution SNR against the outcome SNR of all channels/signal components for each of the subjects. Note that each of the subjects had several channels/signal components with both strong outcome SNR and strong execution SNR. On average, the outcome SNR was significantly higher than execution SNR for all subjects, except for S4 ( $S1\ p < 10^{-17}$ ,  $S2\ p < 10^{-18}$ ,  $S3\ p < 10^{-3}$ ,  $S4\ p = 0.94$ , all subjects pooled  $p < 10^{-38}$ , Mann–Whitney–Wilcoxon test). For every subject, at least one channel could be found with outcome SNR of 0.93 or higher (highest SNRs—S1: 1.26, S2: 1.18, S3: 1.02, S4: 0.93) and with execution SNR of 0.50 or higher (highest SNRs—S1: 0.54, S2: 0.84, S3: 0.63, S4: 0.50). Importantly, for each subject a large number of electrodes with high execution SNRs and/or high outcome SNRs could be found: on average, 68% of channels exhibited a significant ERNR for at least one signal component (average calculated over subjects and signal components). Interestingly, we found strong ERNRs in the low as well as in the high frequency component. For the outcome error, SNR of the low frequency component ( $0.36 \pm 0.01$ ) had a tendency to be higher than the SNR of the high frequency component ( $0.35 \pm 0.01$ ;  $p = 0.054$ , Mann–Whitney–Wilcoxon test). In the case

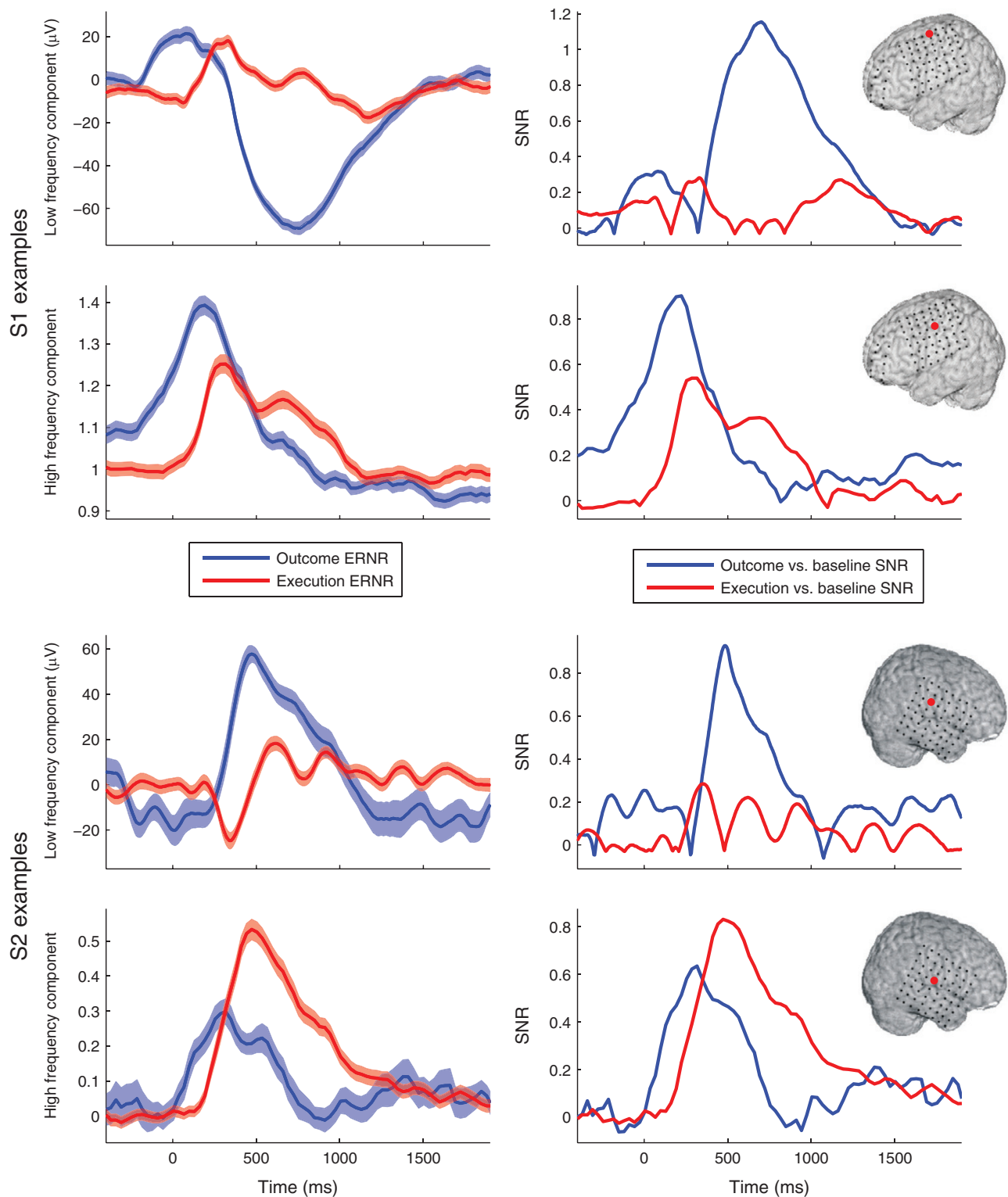


**Figure 6.** Example of two channels for S1 and two channels for S2 that could be used to detect both execution and outcome errors and differentiate between them. Channels selected as examples are shown as red dots on the small depictions of subjects' brains on the right side. Left panels show outcome ERNR (blue) and execution ERNR (red) as mean  $\pm$  sem. Right panels show outcome versus baseline SNR (blue) and execution versus baseline SNR (red) for both channels. For both subjects the channel shown in the top panel exhibited a strong outcome ERNR, while the channel in the bottom panel exhibited a strong outcome ERNR and a strong execution ERNR.

of the execution error, SNR of the low frequency component ( $0.207 \pm 0.005$ ) was significantly higher than the SNR of the high frequency component ( $0.206 \pm 0.007$ ;  $p < 0.05$ , Mann–Whitney–Wilcoxon test).

Differences between outcome and execution ERNRs on the single channel and signal component were investigated by looking at the outcome versus execution SNR. For every subject we found at least one channel and signal component

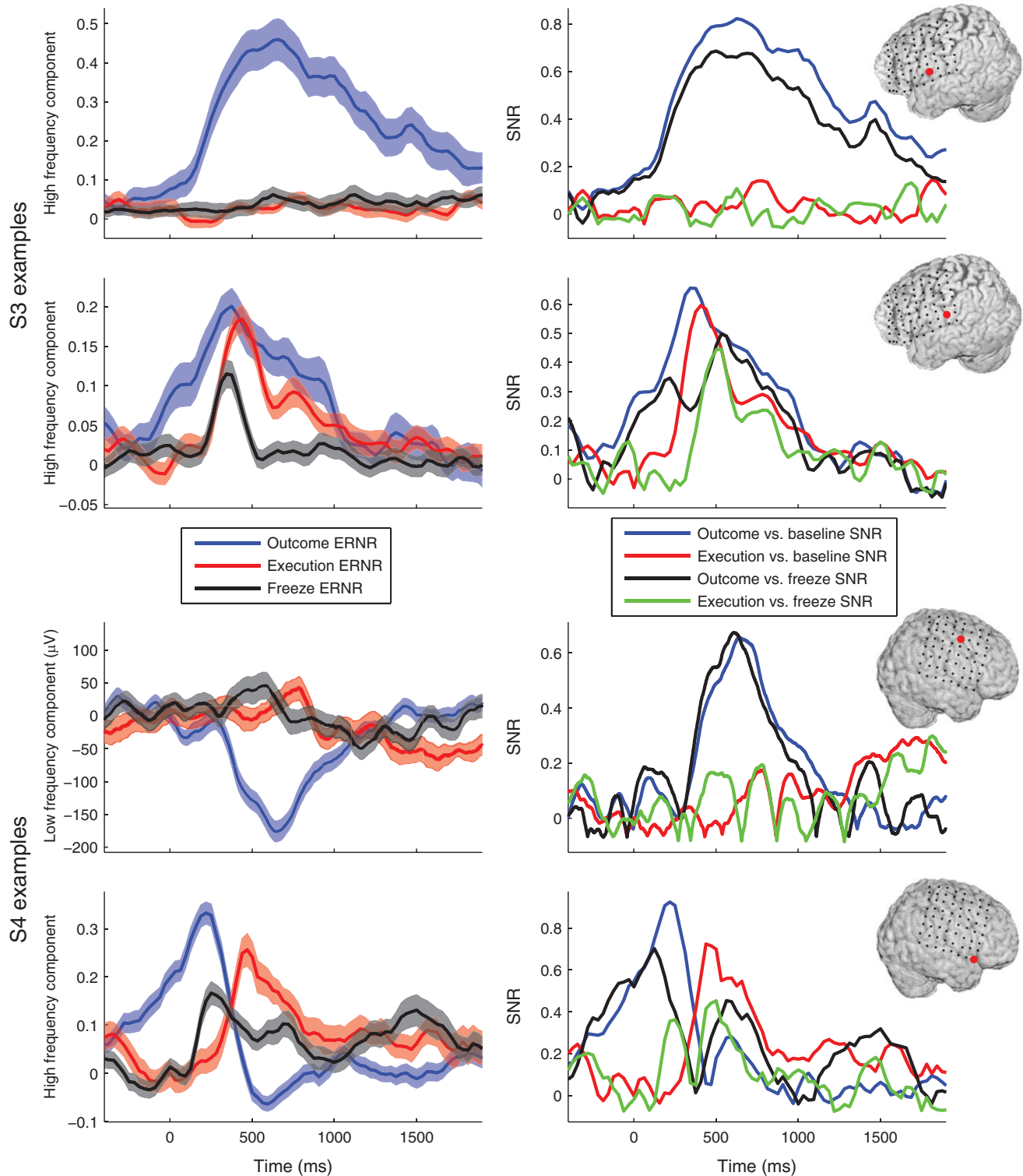


**Figure 7.** Example of two channels for S3 and two channels for S4 that could be used to detect both execution and outcome errors and differentiate between them. Channels selected as examples are shown as red dots on the depictions of the subjects' brains on the right. Left panels show outcome ERNR (blue), execution ERNR (red) and freeze neuronal response (black) as mean  $\pm$  sem. Right panels show outcome versus baseline SNR (blue), execution versus baseline SNR (red), outcome versus freeze SNR (black) and execution versus freeze SNR (green). For S3, the channel shown in the top panel exhibited a strong outcome ERNR, while the channel in the bottom panel exhibited a strong outcome ERNR and a strong execution ERNR. In the case of S4, the channel in the top panel exhibited a strong outcome ERNR, while the channel in the bottom panels exhibited a strong outcome ERNR and a strong execution ERNR.

that showed outcome versus execution SNR of 0.70 or higher (maximum outcome versus execution SNR—S1: 1.05, S2: 0.83, S3: 0.81, S4: 0.70).

We also investigated whether low and high frequency components from the same electrode contained independent information about errors. Figure 9 shows scatter plots of the



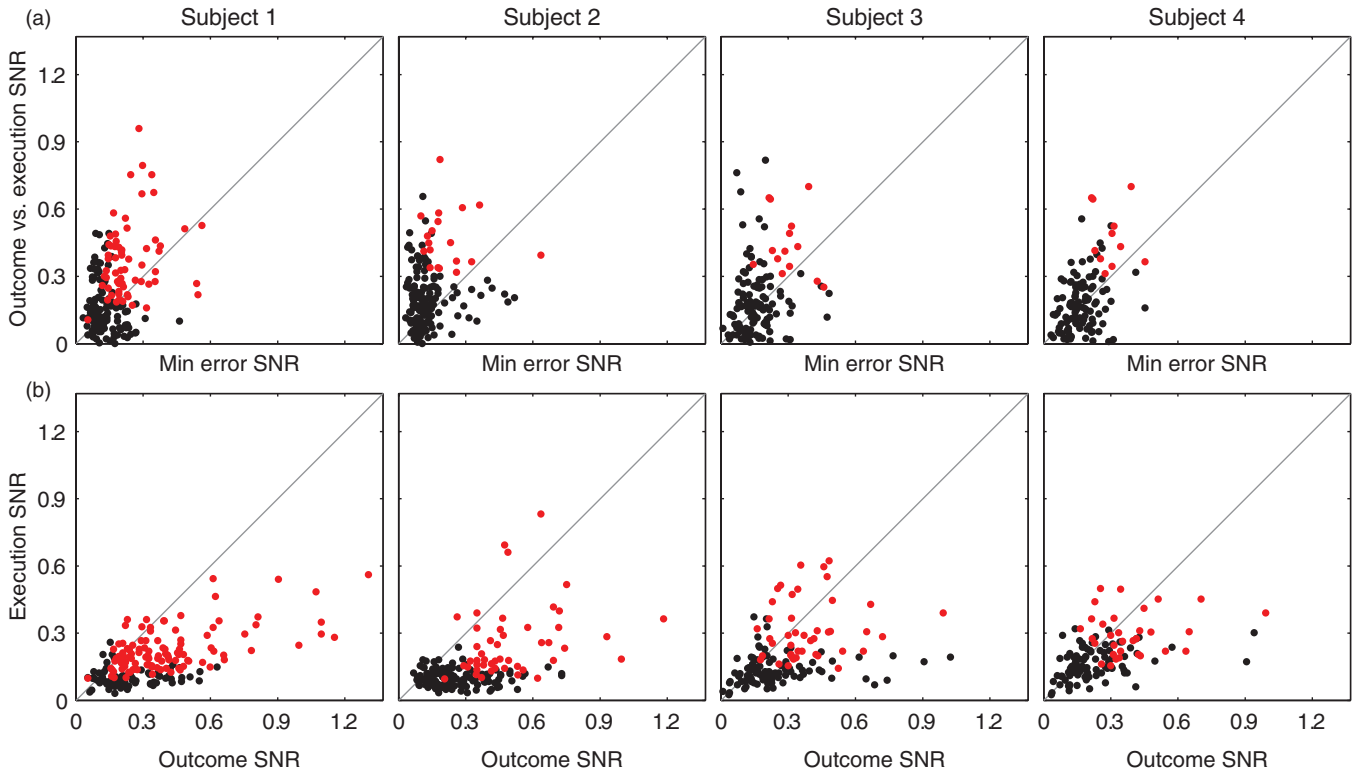


**Figure 8.** (a) A scatter plot showing outcome versus execution SNR against the minimum between outcome SNR and execution SNR (min error SNR). One dot represents one signal component of one channel. Red dots depict channels/signal components with a significant outcome, execution and outcome versus execution SNR. (b) A scatter plot showing execution SNR against outcome SNR. Red dots depict channels/signal components that had both significant outcome ERNR and execution ERNR.

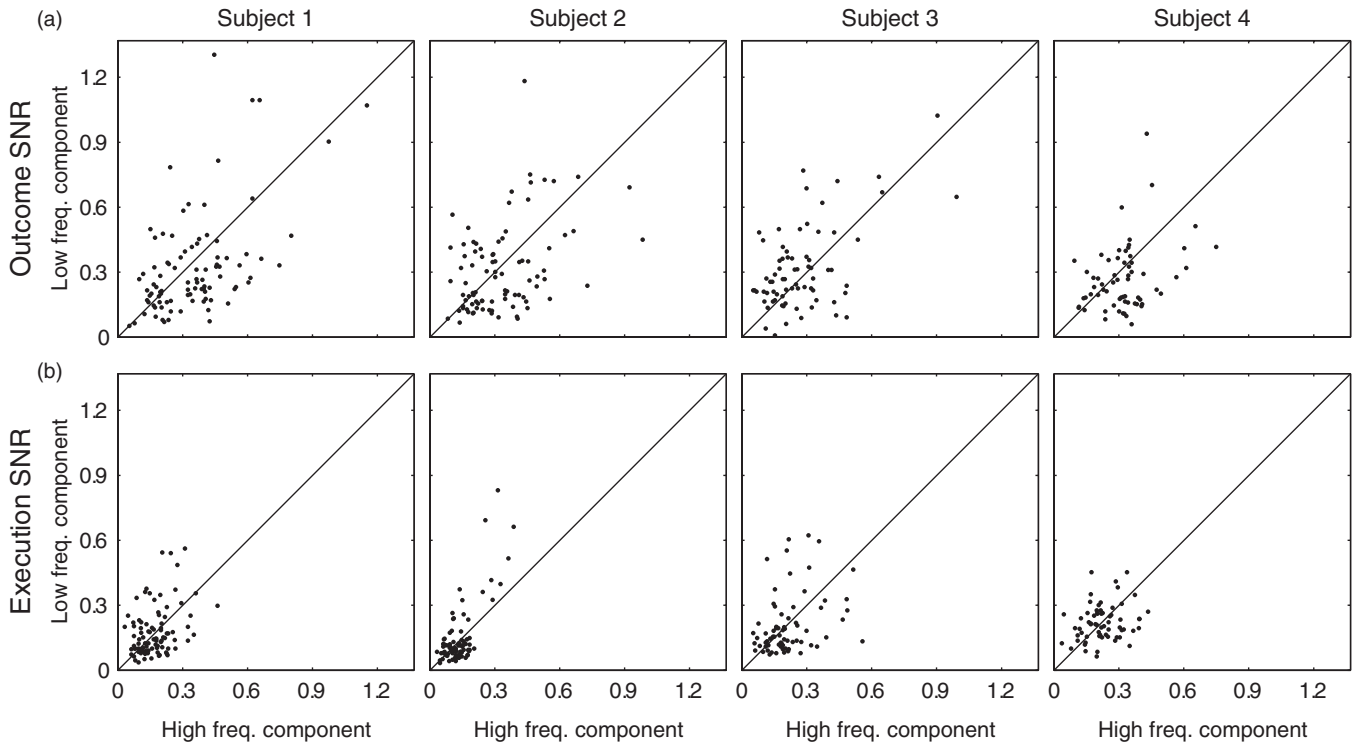
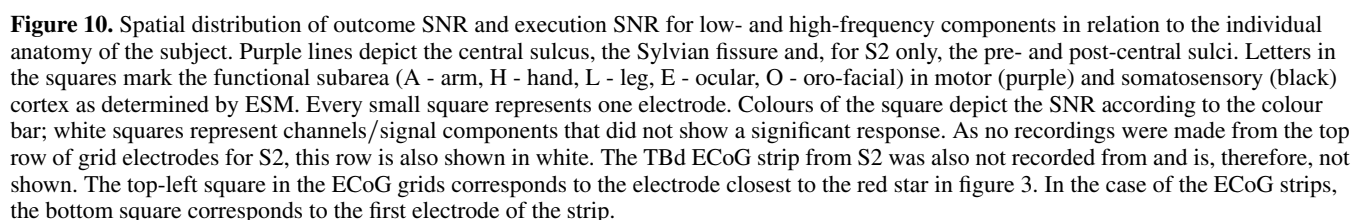


**Figure 9.** A scatter plot showing the low-frequency component SNR against the high-frequency component SNR. Results are shown separately for outcome ERNR (a) and for execution ERNR (b). One dot represents one channel.

low frequency component SNR versus the high frequency components SNR of the same channel. For every subject one

can find channels that are far from the diagonal, indicating that low and high frequency components can be used as partially



somatosensory or other using the ESM (described in section 2). For outcome error, 70% of the motor, 70% of the somatosensory and 60% of the electrodes from other areas showed a significant ERNR (table 2). For execution errors, the proportions were: 50% for motor, 44% for somatosensory and 38% for other areas (table 3). There were no significant differences in the proportions of the electrodes with significant

Next we investigated in which cortical areas ERNRs could be found (figure 10). Electrodes were classified as motor,

**Table 2.** Number and proportion of electrodes with significant outcome ERNR (see section 2 for details of significance criteria). For each of the subjects, electrodes were pooled across two signal components (low and high frequency bands). In the bottom row, electrodes were additionally pooled across subjects.

|        | Motor |          | Somatosensory |         | Other |           |
|--------|-------|----------|---------------|---------|-------|-----------|
| S1     | 93%   | (41/44)  | 89%           | (32/36) | 85%   | (88/104)  |
| S2     | 50%   | (3/6)    | 50%           | (2/4)   | 52%   | (87/166)  |
| S3     | 61%   | (22/36)  | 55%           | (12/22) | 44%   | (38/86)   |
| S4     | 45%   | (10/22)  | 61%           | (17/28) | 58%   | (45/78)   |
| Pooled | 70%   | (76/108) | 70%           | (63/90) | 59%   | (258/434) |

**Table 3.** Number and proportion of electrodes with significant execution ERNR. See table 2 caption for details.

|        | Motor |          | Somatosensory |         | Other |           |
|--------|-------|----------|---------------|---------|-------|-----------|
| S1     | 68%   | (30/44)  | 72%           | (26/36) | 59%   | (61/104)  |
| S2     | 50%   | (3/6)    | 50%           | (2/4)   | 41%   | (68/166)  |
| S3     | 50%   | (18/36)  | 41%           | (9/22)  | 30%   | (26/86)   |
| S4     | 14%   | (3/22)   | 11%           | (3/28)  | 13%   | (10/78)   |
| Pooled | 50%   | (54/108) | 44%           | (40/90) | 38%   | (165/434) |

ERNR between the motor and somatosensory areas for both error types ( $p > 0.47$ , Fisher's exact test) and between somatosensory and other areas ( $p > 0.07$ , Fisher's exact test). Proportion of electrodes with significant ERNR was significantly higher for motor area compared to other areas for both error types ( $p < 0.05$ , Fisher's exact test). For both error types, the average SNRs of electrodes showing significant responses (outcome error: motor SNR  $0.46 \pm 0.02$ , somatosensory SNR  $0.46 \pm 0.03$ , SNR of other areas  $0.40 \pm 0.01$ ; execution error: motor SNR  $0.29 \pm 0.02$ , somatosensory SNR  $0.28 \pm 0.02$ , SNR of other areas  $0.24 \pm 0.01$ ) was not significantly different ( $p > 0.81$ , Mann–Whitney–Wilcoxon test) between motor and somatosensory areas for both error types and was significantly higher for motor compared to other areas ( $p < 0.05$ , Mann–Whitney–Wilcoxon test) and for somatosensory compared to other areas ( $p < 0.05$ , Mann–Whitney–Wilcoxon test).

In motor (somatosensory) cortex outcome SNR was above 0.62 (0.65) while execution SNR was above 0.18 (0.18) for at least one electrode in each subject. S2 had a poor coverage of motor cortex with only three electrodes recording from that area (see figure 2). Disregarding this subject increased the minimum SNR values to 0.62 (0.73) for outcome error and 0.40 (0.41) for execution error. Therefore, it was always possible to find electrodes with significant ERNR with SNR above 0.40 in motor cortex for both outcome and execution error if the electrode grid had a good coverage of the motor cortex.

In addition, we found outcome versus execution SNR of 0.53 or higher for at least one channel and signal component in the motor cortex (S1: 1.05, S2: 0.65, S3: 0.76, S4: 0.54) and 0.50 or higher for at least one channel and signal component in the somatosensory cortex (S1: 0.81, S2: 0.54, S3: 0.81, S4: 0.50) for every subject. Therefore, outcome and execution ERNRs in the motor cortex are not only different from baseline, but one can also find electrodes where these ERNRs are different from each other.

**Table 4.** Number, percentage and SNR (average  $\pm$  standard deviation) of electrodes with significant responses, separately for electrodes recording from different subareas of motor cortex (see section 2 for details of significance criteria). Anatomical information was gained from ESM (see section 2 for details). Electrodes were pooled over subjects and frequency components.

|            | Outcome error |                 | Execution error |                 |
|------------|---------------|-----------------|-----------------|-----------------|
|            | Per cent      | SNR             | Per cent        | SNR             |
| Hand       | 61% (11/18)   | $0.42 \pm 0.12$ | 61% (11/18)     | $0.29 \pm 0.11$ |
| Arm        | 80% (16/20)   | $0.50 \pm 0.19$ | 60% (12/20)     | $0.28 \pm 0.12$ |
| Ocular     | 93% (13/14)   | $0.42 \pm 0.25$ | 57% (8/14)      | $0.29 \pm 0.12$ |
| Oro-facial | 68% (38/56)   | $0.40 \pm 0.20$ | 38% (21/56)     | $0.26 \pm 0.09$ |
| Leg        | 100% (6/6)    | $0.63 \pm 0.36$ | 83% (5/6)       | $0.27 \pm 0.09$ |

**Table 5.** Number, percentage and SNR (average  $\pm$  standard deviation) of electrodes with significant responses, separately for electrodes recording from different subareas of somatosensory cortex. See table 4 caption for details.

|            | Outcome error |                 | Execution error |                 |
|------------|---------------|-----------------|-----------------|-----------------|
|            | Per cent      | SNR             | Per cent        | SNR             |
| Hand       | 72% (36/50)   | $0.49 \pm 0.19$ | 58% (29/50)     | $0.33 \pm 0.13$ |
| Arm        | 79% (11/14)   | $0.37 \pm 0.06$ | 14% (2/14)      | $0.27 \pm 0.08$ |
| Oro-facial | 61% (17/28)   | $0.44 \pm 0.18$ | 25% (7/28)      | $0.24 \pm 0.06$ |

We also compared the ERNR strength of different functional subareas of the motor and somatosensory cortex. To this end, the percentage of electrodes exhibiting a significant ERNR and the average SNRs of these electrodes were computed for the different subareas (tables 4 and 5). Responses were pooled over frequency components. Therefore, each electrode was counted twice. For motor and somatosensory cortex no significant differences in the SNRs or in the electrode proportions between the subareas were found, neither for outcome nor for execution error (Fisher's exact test to compare proportions; Mann–Whitney–Wilcoxon test to compare SNRs) after the correction for the multiple testing (Benjamini–Hochberg procedure with false discovery rate of 5%).

### 3.5. Classification analysis

We investigated how well outcome or execution ERNRs can be differentiated from baseline activity on a single trial basis (see section 2.4.6 for methodological details). Signals from single electrodes were already information-rich enough to obtain high classification accuracies (figure 11). For each subject and both errors at least one electrode existed which yielded an accuracy of 80% or higher (outcome error—S1: 0.85, S2: 0.91, S3: 0.85, S4: 0.80; execution error—S1: 0.88, S2: 0.86, S3: 0.83, S4: 0.88; figure 11). When signals from all motor electrodes were used, decoding accuracy remained high, 77% or higher, except for execution ERNRs for S2 (outcome error—S1: 0.97, S2: 0.79, S3: 0.79, S4: 0.86; execution error—S1: 0.77, S2: 0.60, S3: 0.92, S4: 0.80).

Next, we classified outcome versus execution ERNR on a single-trial basis (see section 2.4.6 for methodological details). Again, high classification accuracies could be obtained with signals from single electrodes (figure 12), where for each

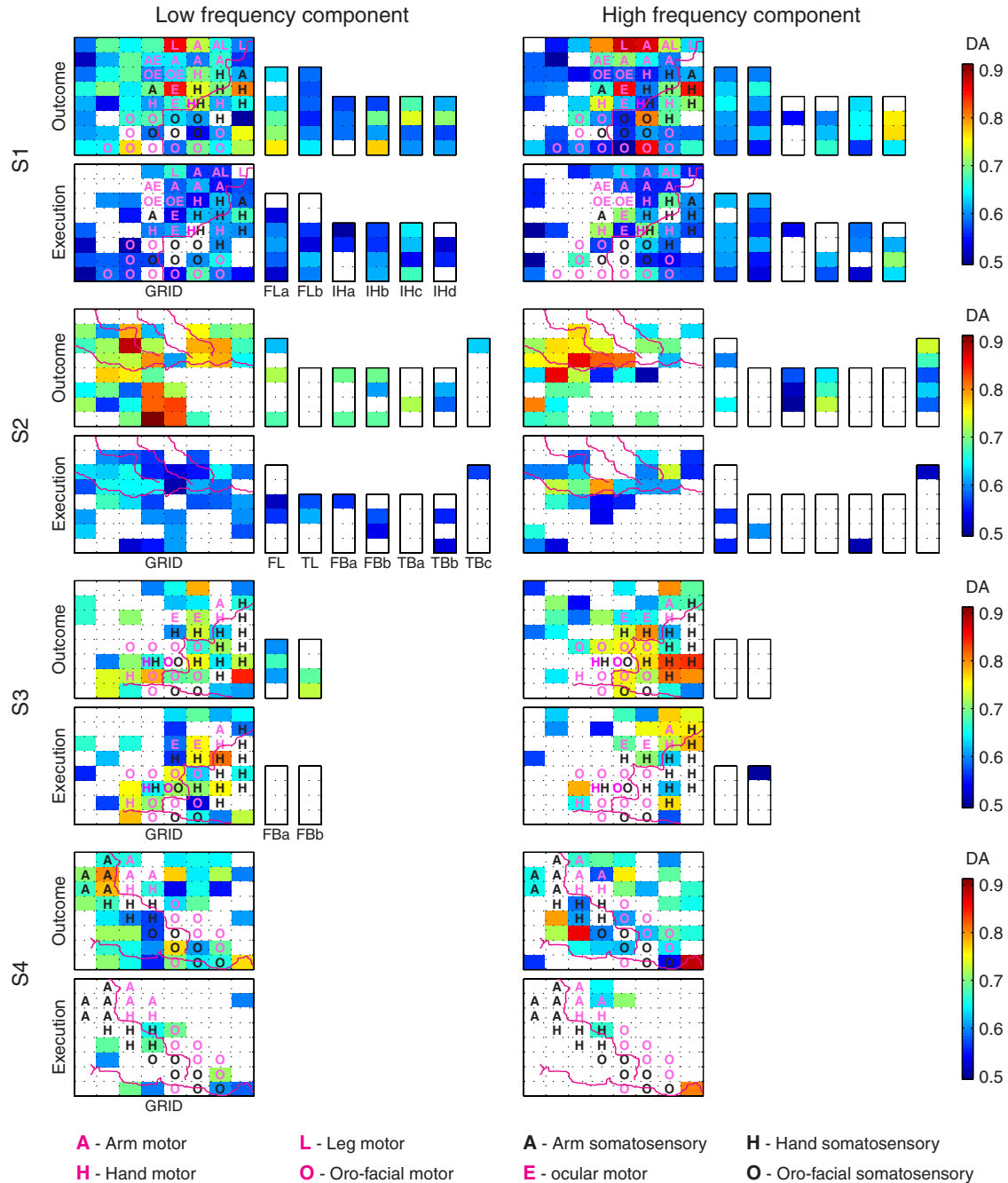


**Figure 11.** Spatial distribution of DA of classifying outcome SNR against baseline and execution SNR against baseline for low- and high-frequency components in relation to the individual anatomy of the subject (see the caption to figure 10 for details). Colours of the squares depict the DA according to the colour bar.

subject at least one electrode yielded an accuracy of 83% or higher (S1: 0.87, S2: 0.88, S3: 0.83, S4: 0.85; figure 12). When signals from all motor electrodes were used, decoding accuracy remained high, at 76% or higher (S1: 0.97, S2: 0.76, S3: 0.83, S4: 0.80).

#### 4. Discussion

In this study we showed that neural correlates of outcome and execution errors can be found in ECoG recordings from the motor, somatosensory, parietal, temporal and pre-frontal

cortex. For each subject we found channels which can be used to differentiate outcome and execution errors from the baseline activity and to differentiate between the two error types.

We observed neuronal responses to errors both in the low pass filtered ECoG signal and in the high gamma activity. ERNRs in low pass filtered signals have been found before in a large number of EEG (for review see Bechtereva *et al* 2005, van Veen and Carter 2006, Jocham and Ullsperger 2009), MEG (Koelewijn *et al* 2008) studies. Jung *et al* (2010) discovered ERNRs in high frequency activity. In that study intracortical stereoencephalography (SEEG) was used a



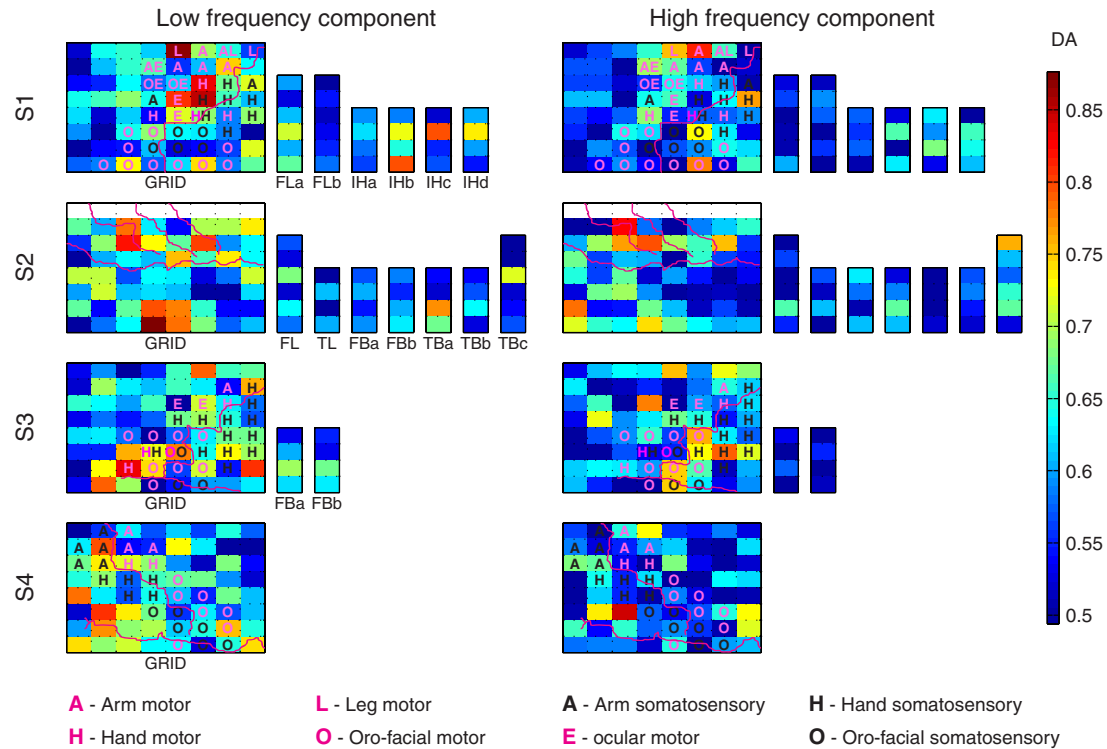


**Figure 12.** Spatial distribution of DA of classifying outcome SNR against execution SNR for low- and high-frequency components in relation to the individual anatomy of the subject (see caption to figure 10 for details). Colours of the squares depict the DA according to the colour bar.

method that measures field potentials in the cortex, in contrast to our method (ECoG) which records field potentials from the cortical surface.

In addition, we showed that the low and high frequency signal components of the same electrode can carry partially independent information about the errors, as for many electrodes only one of the components showed a strong response to one of the errors, while the other component did not. Therefore, low and high frequency components of the ERNR might be used in conjunction for error detection and discrimination. Moreover, we observed a wide distribution of error response strength across different cortical areas. For both error types, there was at least one electrode per subject yielding a high SNR (0.93 or higher for outcome error and 0.50 or higher for execution error) and more than half of the recorded electrodes exhibited a significant ERNR. In addition, decoding analysis revealed that, based on signals from single electrodes, one can decode outcome or execution ERNR from the baseline activity at the level of 80% or higher. This implies widespread neuronal responses to error events. However, not all responses were specific to only one type of error. Reconstruction of the electrode locations demonstrated that, for every subject and for both error types, at least one electrode exhibited a strong ( $\text{SNR} > 0.40$ ) ERNR over the motor cortex. Furthermore, decoding outcome or execution ERNR from the baseline activity, using only channels over the motor cortex, was possible with DA of 77%. An exception was the execution error for S2 where, due to the placement of the implant and more conservative electrode selection criteria, only three electrodes were located over the motor cortex and a DA of only 60% was

reached. An implant position similar to those of other subjects would have provided more electrodes over the motor cortex and, thus, might have provided recordings of more informative signals.

We also investigated the differences between outcome and execution ERNRs. For every subject, it was possible to find an electrode with outcome versus execution SNR of 0.53 or higher. In addition, for every subject, outcome and execution ERNRs could be decoded with DA of at least 76%. If we exclude S2, which had a poor coverage of motor cortex, each subject had a channel with DA of 80% or above. These results show that it is possible to decode outcome and execution ERNRs between each other and against baseline activity.

Screen freeze events were used as a control for specific visual stimuli in the case of outcome ERNR and as a control for the surprise in the case of execution ERNR. This control was not present for the first two subjects. Thus, one might speculate that outcome and execution average SNR for the first two subjects would not be as high, had the freeze event been included as a control event, as it was for the last two subjects. This was, however, not the case: for the outcome error no significant differences were found between the average SNRs (first two subjects: average SNR  $0.48 \pm 0.04$ , last two subjects: average SNR  $0.43 \pm 0.03$ ,  $p = 0.41$ , Mann–Whitney–Wilcoxon test). In the case of execution error the average SNR of the last two subjects was even significantly higher than for the first two subjects (first two subjects: average SNR  $0.26 \pm 0.02$ , last two subjects: average SNR  $0.34 \pm 0.03$ ,  $p < 0.01$ , Mann–Whitney–Wilcoxon test). Therefore, we conclude (1) that including the freeze event control improved

the sensitivity of ERNR detection and (2) that the SNRs of outcome and execution error of the first two subjects were representative as well, even though the freeze control was missing.

#### 4.1. Spectro-temporal characteristics of neuronal error responses

Following an error event, one can observe stereotypical spectral responses in which the amplitude in very low frequencies (0–4 Hz) and in high gamma frequencies (above 40 Hz) is increased in relation to the baseline (figure 4). We found that changes in the low frequencies can better be described using the low pass filtered signal, since in that case phase information is included as well. The high gamma response was present in a wide frequency band where amplitudes changed across many frequencies homogeneously. Therefore, computing the average amplitudes over these frequencies yields a less noisy response. We chose a frequency band from 60 to 200 Hz because this band exhibited common behaviour across subjects, channels and error events (supplementary figure 2 available from [stacks.iop.org/JNE/9/026007/mmedia](http://stacks.iop.org/JNE/9/026007/mmedia)). For subjects S1 and S2 the upper boundary of the high frequency band was limited to 128 Hz due to the sampling frequency of the recording amplifier.

Jung *et al* (2010) studied intracortical SEEG signals in a reaction time task where negative feedback was given if timing requirements were not met. They reported high gamma neuronal responses with similar spectro-temporal characteristics as we found in response to outcome and execution errors in our continuous control task. Even though task and recording method were both different, neuronal responses are, in essence, error event neuronal responses and could, therefore, be related.

On the other hand, neuronal responses to non-error events can also exhibit similar spectro-temporal characteristics: onset of arm movements (Ball *et al* 2009b), self-paced individual finger movements (Kubanek *et al* 2009, Miller *et al* 2009, Wang *et al* 2009), thumb button press (Crone *et al* 2006), hand movements (Leuthardt *et al* 2004, Wisneski *et al* 2008), tongue, fist and foot isometric contraction (Crone *et al* 1998a, 1998b), onset of auditory stimuli (Crone *et al* 2001, Ray *et al* 2008, Boatman-Reich *et al* 2010), tactile stimulus (Ray *et al* 2008), face recognition (Lachaux *et al* 2003), attention and short-term memory (Jensen *et al* 2007), mental calculation (Vansteensel *et al* 2010) and word recognition (Jerbi *et al* 2009). To test how well ERNRs can be differentiated from all such non-error events, further ECoG experiments with freely behaving subjects, where ERNRs can be compared to neuronal responses to other events, have to eventually be conducted. Such differentiation may be possible as ERNRs could be evoked on different electrodes and exhibit different time courses compared to neural responses to non-error events. This is supported by our finding of different ERNRs to different types of errors (outcome and execution) and by different responses to different non-error events in some of the before-mentioned studies (Ball *et al* 2009b, Wang *et al* 2009, Boatman-Reich *et al* 2010).

#### 4.2. Comparison to previous ERNR studies and widespread ERNR

ERNRs have previously been reported over motor cortex in the low frequency range (0–4 Hz; van Schie *et al* 2004) using EEG recordings and in the beta (15–23 Hz) range (Koelewijn *et al* 2008) using MEG recordings. In addition, increased brain activation correlated with execution errors has been reported in the motor cortex using fMRI (Diedrichsen *et al* 2005). In line with these studies, we found strong outcome and execution ERNR in both low and high frequency components of the signal. To the best of our knowledge, our study is the first showing high gamma ERNRs in the motor cortex.

Increased fMRI activation correlated with execution errors has also been reported in the somatosensory cortex (Diedrichsen *et al* 2005). We showed that correlates of execution errors and, moreover, outcome errors are present in electrophysiological signals from somatosensory cortex both in low and high frequency signal components.

Besides in motor and somatosensory cortex, we also found widespread ERNRs to outcome and execution errors in other brain areas, including frontal, parietal and temporal cortex. This is consistent with previous studies. Increased fMRI activation in response to negative feedback was found in dorsolateral pre-frontal cortex (Zanolie *et al* 2008, Jung *et al* 2010), medial pre-frontal cortex (Ullsperger and von Cramon 2003, Zanolie *et al* 2008), orbito-frontal cortex (Walton *et al* 2004, Zanolie *et al* 2008, Jung *et al* 2010), pre-supplementary motor area (Jung *et al* 2010) and insula (Zanolie *et al* 2008, Jung *et al* 2010). Diedrichsen *et al* (2005) found fMRI activations in response to execution errors in multiple parietal areas. In the lateral temporal cortex, responses to errors in identification and memory tasks were found in single-unit activity (Ojemann 2003, Ojemann *et al* 2004). Our task did not have any identification or memory component but it is possible that there are areas in the temporal lobe responsive to errors in general.

Most of the earlier ERNR studies concentrated on the activation of anterior cingulate cortex (ACC) and its functional meaning (for reviews see Bechtereva *et al* 2005, van Veen and Carter 2006, Jocham and Ullsperger 2009). In only one of our four subjects did we have electrodes ( $N = 2$ ) in the vicinity of the ACC. Therefore, we did not investigate the activation of ACC. Involvement of ACC in error processing in our task deserves further clarification by future studies.

We measured the strength of ERNRs of different cortical areas (motor, somatosensory and pooled data from all other areas) by computing the proportion of electrodes exhibiting significant ERNR and the average SNR of these electrodes. Our results show that, for both error types, the proportion of channels with a significant ERNR and their response strength (as quantified by SNR) is not different between motor and somatosensory cortex. Compared to all other cortical areas that were investigated, the response strength of motor cortical ERNRs is significantly higher. By further evaluating ERNRs in different functional subareas of the motor and the somatosensory cortex, we showed that significant ERNRs were present in different functional subareas that we recorded from (hand, arm, ocular, oro-facial). We also found significant

ERNRs in the leg area of the motor cortex. As the leg electrodes were in immediate vicinity of arm electrodes this finding might be explained by ERNRs originating in the arm area and being also picked up on leg electrodes due to spatial spread of the electrical signals. Furthermore, ERNRs on leg motor electrodes were found only in one subject. This makes the statistics of the ERNR activity in the leg motor area much more unreliable than the statistics for the other subareas, where electrodes were available from several patients. Within motor cortex, all functional subareas exhibited the same response strength to outcome errors. For execution errors the response strength was also not different among different motor cortical subareas. The same result was found for the functional subareas of the somatosensory cortex.

One might suspect that some of these ERNRs were caused by movements correlated with error events and, thus, did not directly reflect error-related neuronal responses. To distinguish ERNRs from movement-related responses, we subtracted responses evoked by eye and thumb movements using the best out of linear and nonlinear models relating ECoG signals to these movements (see section 2). Therefore, we conclude that these movements cannot explain the ERNRs we observed.

On the other hand, due to technical and clinical limitations, movements of other parts of the body or the respective muscle activations could not be tracked. Even though such movements did not play a role for the task and, thus, there is no *a priori* reason to expect these movements to be correlated with error events, we cannot completely disprove that parts of the observed neuronal error signals were confounded by such movements.

#### 4.3. Relevance for brain machine interfaces

One motivation for this study was to investigate whether ERNRs can be used to improve the performance of continuous movement BMIs (Serruya et al 2002, Taylor et al 2002, Carmena et al 2003, McFarland and Wolpaw 2005, Hochberg et al 2006, Kim et al 2008, Velliste et al 2008). Our study provides a significant first step in this direction, showing that strong error-related neuronal responses could be found in ECoG recordings during a continuous control paradigm which mimicked a continuous BMI control task. In addition, we demonstrated that it is possible to differentiate between execution (Diedrichsen et al 2005) and outcome (Krigolson et al 2008) errors. These two types of errors provide independent sources of information. Moreover, both of them can be used to improve the performance of the BMI in different ways. An outcome error can be used to correct an error after it has been made (Blankertz et al 2003, Parra et al 2003, Buttfeld et al 2006, Ferrez and del R Millan 2008) and as a critic for a reinforcement learning adaptive algorithm (DiGiovanna et al 2009). An execution error, on the other hand, can be used as a direct indicator of when the decoded trajectory was decoded improperly, thereby providing useful information for adaptive decoding algorithms (Rotermund et al 2006).

Motor cortex is one of the primary target areas for the implantation of electrodes for invasive BMIs. We showed

that strong ERNRs for both error types can be found in motor cortical signals. Therefore, movement decoding and error detection may be implemented using the same electrode implants. Consequently, no additional implants over other cortical areas would be required for BMIs employing such neuronal error signals. This would substantially reduce the burden of implantation for such BMIs.

#### Acknowledgments

This work was supported by the German Federal Ministry of Education and Research (BMBF) grant 01GQ0420 to BCCN Freiburg, by the BMBF GoBio grant 0313891 and by Imperial College London. We would like to thank the epilepsy subjects for participating in our study, Tobias Pistohl and Xiang Liao for help with the experiments and Joerg Fischer for help with our laboratory software. We are grateful to the staff of the Freiburg University Hospital, Epilepsy Center for their help with the epilepsy patients and the recording equipment.

#### References

- Ball T, Kern M, Mutschler I, Aertsen A and Schulze-Bonhage A 2009a Signal quality of simultaneously recorded invasive and non-invasive EEG *Neuroimage* **46** 708–16
- Ball T, Schulze-Bonhage A, Aertsen A and Mehring C 2009b Differential representation of arm movement direction in relation to cortical anatomy and function *J. Neural Eng.* **6** 016006
- Bechtereva N P, Shemyakina N V, Starchenko M G, Danko S G and Medvedev S V 2005 Error detection mechanisms of the brain: background and prospects *Int. J. Psychophysiol.* **58** 227–34
- Benjamini Y and Hochberg Y 1995 Controlling the false discovery rate—a practical and powerful approach to multiple testing *J. R. Stat. Soc. B* **57** 289–300
- Benjamini Y and Yekutieli D 2001 The control of the false discovery rate in multiple testing under dependency *J. R. Stat. Soc. B* **29** 1165–88
- Blankertz B, Dornhege G, Schäfer C, Krepi R, Kohlmorgen J, Müller K-R, Kunzmann V, Losch F and Curio G 2003 Boosting bit rates and error detection for the classification of fast-paced motor commands based on single-trial EEG analysis *IEEE Trans. Neural Syst. Rehabil. Eng.* **11** 127–31
- Blumberg J, Rickert J, Waldert S, Schulze-Bonhage A, Aertsen A and Mehring C 2007 Adaptive classification for brain computer interfaces *Conf. Proc. IEEE Eng. Med. Biol. Soc.* **2007** 2536–9
- Boatman-Reich D, Franaszczuk P J, Korzeniewska A, Caffo B, Ritzl E K, Colwell S and Crone N E 2010 Quantifying auditory event-related responses in multichannel human intracranial recordings *Front. Comput. Neurosci.* **4** 4
- Buttfeld A, Ferrez P and Millán J D 2006 Towards a robust BCI: error potentials and online learning *IEEE Trans. Neural Syst. Rehabil. Eng.* **14** 164–8
- Carmena J M, Lebedev M A, Crist R E, O'Doherty J E, Santucci D M, Dimitrov D F, Patil P G, Henriquez C S and Nicolelis M A 2003 Learning to control a brain-machine interface for reaching and grasping by primates *PLoS Biol.* **1** E42
- Chao Z C, Nagasaka Y and Fujii N 2010 Long-term asynchronous decoding of arm motion using electrocorticographic signals in monkeys *Front. Neuroeng.* **3** 3
- Cooper R, Winter A L, Crow H J and Walter W G 1965 Comparison of subcortical, cortical and scalp activity using chronically



- indwelling electrodes in man *Electroencephalogr. Clin. Neurophysiol.* **18** 217–28
- Crone N E, Boatman D, Gordon B and Hao L 2001 Induced electrocorticographic gamma activity during auditory perception 2001 *Clin. Neurophysiol.* **112** 565–82 [Brazier Award-winning article](#)
- Crone N E, Miglioretti D L, Gordon B and Lesser R P 1998a Functional mapping of human sensorimotor cortex with electrocorticographic spectral analysis: II. Event-related synchronization in the gamma band *Brain* **121** 2301–15
- Crone N E, Miglioretti D L, Gordon B, Sieracki J M, Wilson M T, Uematsu S and Lesser R P 1998b Functional mapping of human sensorimotor cortex with electrocorticographic spectral analysis: I. Alpha and beta event-related desynchronization *Brain* **121** 2271–99
- Crone N E, Sinai A and Korzeniewska A 2006 High-frequency gamma oscillations and human brain mapping with electrocorticography *Prog. Brain Res.* **159** 275–95
- Diedrichsen J, Hashambhoy Y, Rane T and Shadmehr R 2005 Neural correlates of reach errors *J. Neurosci.* **25** 9919–31
- DiGiovanna J, Mahmoudi B, Fortes J, Principe J and Sanchez J 2009 Coadaptive brain–machine interface via reinforcement learning *IEEE Trans. Biomed. Eng.* **56** 54–64
- Efron B and Tibshirani R 1993 *An Introduction to the Bootstrap* (New York: Chapman and Hall)
- Falkenstein M, Hohnsbein J, Hoormann J and Blanke L 1991 Effects of crossmodal divided attention on late ERP components: II. Error processing in choice reaction tasks *Electroencephalogr. Clin. Neurophysiol.* **78** 447–55
- Fan R-E, Chen P-H and Lin C-J 2005 Working set selection using second order information for training support vector machines *J. Mach. Learn. Res.* **6** 1889–918
- Ferrez P and del R Millan J 2008 Error-related EEG potentials generated during simulated brain–computer interaction *IEEE Trans. Biomed. Eng.* **55** 923–9
- Foerster O 1931 The cerebral cortex in man *Lancet* **221** 309–12
- Friedman J H 1989 Regularized discriminant-analysis *J. Am. Stat. Assoc.* **84** 165–75
- Gehring W, Goss B, Coles M, Meyer D and Donchin E 1993 A neural system for error detection and compensation *Psychol. Sci.* **4** 385–90
- Hochberg L R, Serruya M D, Friehs G M, Mukand J A, Saleh M, Caplan A H, Branner A, Chen D, Penn R D and Donoghue J P 2006 Neuronal ensemble control of prosthetic devices by a human with tetraplegia *Nature* **442** 164–71
- Jensen O, Kaiser J and Lachaux J P 2007 Human gamma-frequency oscillations associated with attention and memory *Trends Neurosci.* **30** 317–24
- Jerbi K et al 2009 Task-related gamma-band dynamics from an intracerebral perspective: review and implications for surface EEG and MEG *Hum. Brain Mapp.* **30** 1758–71
- Jocham G and Ullsperger M 2009 Neuropharmacology of performance monitoring *Neurosci. Biobehav. Rev.* **33** 48–60
- Jung J, Jerbi K, Ossandon T, Ryvlin P, Isnard J, Bertrand O, Guenot M, Mauguier F and Lachaux J P 2010 Brain responses to success and failure: direct recordings from human cerebral cortex *Hum. Brain Mapp.* **31** 1217–32
- Kim S P, Simeral J D, Hochberg L R, Donoghue J P and Black M J 2008 Neural control of computer cursor velocity by decoding motor cortical spiking activity in humans with tetraplegia *J. Neural Eng.* **5** 455–76
- Koelewijn T, van Schie H, Bekkering H, Oostenveld R and Jensen O 2008 Motor-cortical beta oscillations are modulated by correctness of observed action *Neuroimage* **40** 767–75
- Kovalev D, Spreer J, Honegger J, Zentner J, Schulze-Bonhage A and Huppertz H J 2005 Rapid and fully automated visualization of subdural electrodes in the presurgical evaluation of epilepsy patients *AJNR Am. J. Neuroradiol.* **26** 1078–83
- Krigolson O, Holroyd C, Van Gyn G and Heath M 2008 Electroencephalographic correlates of target and outcome errors *Exp. Brain Res.* **190** 401–11
- Krusienski D J, Grosse-Wentrup M, Galan F, Coyle D, Miller K J, Forney E and Anderson C W 2011 Critical issues in state-of-the-art brain–computer interface signal processing *J. Neural Eng.* **8** 025002
- Kubaneck J, Miller K J, Ojemann J G, Wolpaw J R and Schalk G 2009 Decoding flexion of individual fingers using electrocorticographic signals in humans *J. Neural Eng.* **6** 066001
- Lachaux J P, Rudrauf D and Kahane P 2003 Intracranial EEG and human brain mapping *J. Physiol. Paris* **97** 613–28
- Leuthardt E C, Schalk G, Wolpaw J R, Ojemann J G and Moran D W 2004 A brain–computer interface using electrocorticographic signals in humans *J. Neural Eng.* **1** 63–71
- McFarland D J and Wolpaw J R 2005 Sensorimotor rhythm-based brain–computer interface (BCI): feature selection by regression improves performance *IEEE Trans. Neural. Syst. Rehabil. Eng.* **13** 372–9
- Mehring C, Rickert J, Vaadia E, Cardosa de Oliveira S, Aertsen A and Rotter S 2003 Inference of hand movements from local field potentials in monkey motor cortex *Nat. Neurosci.* **6** 1253–4
- Miller K J, Zanos S, Fetz E E, den Nijs M and Ojemann J G 2009 Decoupling the cortical power spectrum reveals real-time representation of individual finger movements in humans *J. Neurosci.* **29** 3132–7
- Miltner W H R, Braun C H and Coles M G H 1997 Event-related brain potentials following incorrect feedback in a time-estimation task: evidence for a ‘generic’ neural system for error detection *J. Cogn. Neurosci.* **9** 788–98
- Ojemann G 2003 The neurobiology of language and verbal memory: observations from awake neurosurgery *Int. J. Psychophysiol.* **48** 141–6
- Ojemann G, Schoenfield-McNeill J and Corina D 2004 Different neurons in different regions of human temporal lobe distinguish correct from incorrect identification or memory *Neuropsychologia* **42** 1383–93
- Parra L, Spence C, Gerson A and Sajda P 2003 Response error correction—a demonstration of improved human–machine performance using real-time EEG monitoring *IEEE Trans. Neural Syst. Rehabil. Eng.* **11** 173–7
- Pistohl T, Ball T, Schulze-Bonhage A, Aertsen A and Mehring C 2008 Prediction of arm movement trajectories from ECoG-recordings in humans *J. Neurosci. Methods* **167** 105–14
- Ray S, Niebur E, Hsiao S S, Sinai A and Crone N E 2008 High-frequency gamma activity (80–150 Hz) is increased in human cortex during selective attention *Clin. Neurophysiol.* **119** 116–33
- Rotermund D, Ernst U and Pawelzik K 2006 Towards on-line adaptation of neuro-prostheses with neuronal evaluation signals *Biol. Cybern.* **95** 243–57
- Savitzky A and Golay M J E 1964 Smoothing and differentiation of data by simplified least squares procedures *Anal. Chem.* **36** 1627–39
- Schafer R W 2011 What is a Savitzky–Golay filter? *IEEE Signal Process. Mag.* **28** 111–7
- Schalk G, Kubaneck J, Miller K J, Anderson N R, Leuthardt E C, Ojemann J G, Limbrick D, Moran D, Gerhardt L A and Wolpaw J R 2007 Decoding two-dimensional movement trajectories using electrocorticographic signals in humans *J. Neural Eng.* **4** 264–75
- Schalk G, Wolpaw J R, McFarland D J and Pfurtscheller G 2000 EEG-based communication: presence of an error potential *Clin. Neurophysiol.* **111** 2138–44



- Serruya M D, Hatsopoulos N G, Paninski L, Fellows M R and Donoghue J P 2002 Instant neural control of a movement signal *Nature* **416** 141–2
- Steinier J, Termonia Y and Deltour J 1972 Smoothing and differentiation of data by simplified least square procedure *Anal. Chem.* **44** 1906–9
- Taylor D M, Tillery S I and Schwartz A B 2002 Direct cortical control of 3D neuroprosthetic devices *Science* **296** 1829–32
- Uematsu S, Lesser R, Fisher R S, Gordon B, Hara K, Krauss G L, Vining E P and Webber R W 1992 Motor and sensory cortex in humans: topography studied with chronic subdural stimulation *Neurosurgery* **31** 59–71 discussion 71–52
- Ullsperger M and von Cramon D Y 2003 Error monitoring using external feedback: specific roles of the habenular complex, the reward system, and the cingulate motor area revealed by functional magnetic resonance imaging *J. Neurosci.* **23** 4308–14
- van Schie H T, Mars R B, Coles M G and Bekkering H 2004 Modulation of activity in medial frontal and motor cortices during error observation *Nat. Neurosci.* **7** 549–54
- Vansteensel M J, Hermes D, Aarnoutse E J, Bleichner M G, Schalk G, van Rijen P C, Leijten F S and Ramsey N F 2010 Brain–computer interfacing based on cognitive control *Ann. Neurol.* **67** 809–16
- van Veen V and Carter C S 2006 Error detection, correction, and prevention in the brain: a brief review of data and theories *Clin. EEG Neurosci.* **37** 330–5
- Velliste M, Perel S, Spalding C, Whitford A and Schwartz A 2008 Cortical control of a prosthetic arm for self-feeding *Nature* **453** 1098–101
- Walton M E, Devlin J T and Rushworth M F 2004 Interactions between decision making and performance monitoring within prefrontal cortex *Nat. Neurosci.* **7** 1259–65
- Wang W et al 2009 Human motor cortical activity recorded with micro-ECoG electrodes, during individual finger movements *Conf. Proc. IEEE Eng. Med. Biol. Soc.* **2009** 586–9
- Wisneski K J, Anderson N, Schalk G, Smyth M, Moran D and Leuthardt E C 2008 Unique cortical physiology associated with ipsilateral hand movements and neuroprosthetic implications *Stroke* **39** 3351–9
- Zanolie K, Van Leijenhorst L, Rombouts S A and Crone E A 2008 Separable neural mechanisms contribute to feedback processing in a rule-learning task *Neuropsychologia* **46** 117–26